

AMERICAN UNIVERSITY OF BEIRUT

ASSESSING THE IMPACT OF EXPRESSING ONCOGENIC
BCR-ABL ON HEMATOPEISIS AND INNATE IMMUNITY IN
DROSOPHILA MELANOGASTER

by
DANA MAHMOUD ABUBAKER

A thesis
submitted in partial fulfillment of the requirements
for the degree of Master of Science
to the Department of Experimental Pathology, Immunology and Microbiology
of the Faculty of Medicine
at the American University of Beirut

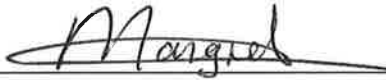
Beirut, Lebanon
August 2019

AMERICAN UNIVERSITY OF BEIRUT

ASSESSING THE IMPACT OF EXPRESSING ONCOGENIC
BCR-ABL ON HEMATOPEISIS AND INNATE IMMUNITY IN
DROSOPHILA MELANOGASTER

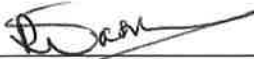
by
DANA MAHMOUD ABUBAKER

Approved by:



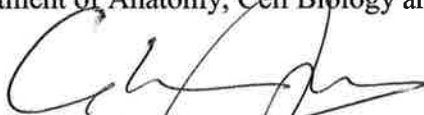
Margret Shirinian, PhD, Assistant Professor
Department of Experimental Pathology, Immunology and Microbiology

Advisor



Rihab Nasr, PhD, Associate Professor
Department of Anatomy, Cell Biology and Physiological Sciences

Co-advisor



Ghassan Matar, PhD, Professor and Chairperson
Department of Experimental Pathology, Immunology and Microbiology

Member of Committee



Elias Rahal, PhD, Associate Professor
Department of Experimental Pathology, Immunology and Microbiology

Member of Committee

Date of thesis defense: August 28, 2019

AMERICAN UNIVERSITY OF BEIRUT

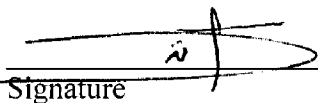
THESIS, DISSERTATION, PROJECT RELEASE FORM

Student Name: ABUBAKER DANA MAHMOUD
Last First Middle

Master's Thesis Master's Project Doctoral Dissertation

I authorize the American University of Beirut to: (a) reproduce hard or electronic copies of my thesis, dissertation, or project; (b) include such copies in the archives and digital repositories of the University; and (c) make freely available such copies to third parties for research or educational purposes.

I authorize the American University of Beirut, to: (a) reproduce hard or electronic copies of it; (b) include such copies in the archives and digital repositories of the University; and (c) make freely available such copies to third parties for research or educational purposes after: **One --- year from the date of submission of my thesis, dissertation, or project.**
Two --- years from the date of submission of my thesis, dissertation, or project.
Three -✓--- years from the date of submission of my thesis, dissertation, or project.


Signature

September 2nd, 2019
Date

ACKNOWLEDGMENTS

To begin with, I would like to thank my thesis advisors, Dr. Margret Shirinian and Dr. Rihab Nasr. I am grateful for your guidance, help and advice throughout this journey. Thank you for always being there and welcoming me into your offices with a smile regardless of how busy you were. I would like to thank, Dr. Elias Rahal and Dr. Ghassan Matar for their continuous support and fruitful discussions. To my advisors and committee members, thank you for always encouraging me to be a better scientist and to seize every chance to learn and grow.

To MS and RN lab members; Amani, Felice, Joy, Ghada and Farah thank you for your continuous help and support. Your help has been vital for the completion of this project. I would also extend many thanks to Dr. Abdou Akkouche and Dr. Wael Bazzi for their support and insightful discussions during this project.

To my second family in Lebanon and irreplaceable friends; Diana, Joelle, Mirna and Zeinab. Thank you for every word of encouragement, every gesture to help and for every fun moment we shared together. Our friendship will always be very close to my heart.

My utmost gratitude goes to my number one supporter; my family. Dad, Mom, Ahmad and Yazeed, this would have never been possible without you. Thank you for bearing with my endless hours of videocalls. Thank you for supporting me through every step of the way. Thank you for always pushing me forward through the ups and downs of this journey.

Thank you, God, for your many blessings during this journey.

AN ABSTRACT OF THE THESIS OF

Dana Mahmoud Abubaker

for Master of Science

Major: Microbiology and Immunology

Title: Assessing the impact of expressing oncogenic *BCR-ABL* on hematopoiesis and innate immunity in *Drosophila melanogaster*

Introduction: CML is caused by a chromosomal translocation resulting in the formation of *BCR-ABL* fusion gene that encodes a constitutively active BCR-ABL tyrosine kinase which activates multiple signal transduction pathways leading to a myeloproliferative disorder in the bone marrow. Some mutations of the oncogene, especially the substitution of threonine with isoleucine on the 315th residue (T315I mutation) of the ABL kinase, have proven resistant to conventional CML therapy; tyrosine kinase inhibitors (TKI). Transgenic flies harboring wildtype *BCR-ABL* (P210) and *BCR-ABL* (T315I) mutants have been generated and tested for their oncogenic potential in a previous study by our group. In this current work, we aimed to investigate the effect of expressing oncogenic *BCR-ABL* on *D. melanogaster* hematopoiesis and innate immunity to better understand the impact of this oncogene in the etiology of CML disease in an *in vivo* model.

Methods: *BCR-ABL*^{P210} and *BCR-ABL*^{T315I} were expressed in *Drosophila* circulating hemocytes which are comparable to mammalian macrophages and bone marrow niche by using the *Hemolectin Delta; UAS-GFP (Hml Δ-Gal4; UAS-GFP)* driver. The transgene expression was validated by immunofluorescence. Following the overexpression, an analysis of the hematopoietic system was performed by assessing changes in circulating hemocytes and GFP positive cells using hemocytometer and flow cytometry. Moreover, given the cellular role the hemocytes play in the innate immunity in *Drosophila melanogaster*, the expression of *drosomycin*, *diptericin* and *Tot A*, respective indicators of Toll, IMD and JAK/STAT; the three-major fly humoral immune pathways, were assessed by real time PCR.

Results: *BCR-ABL*^{P210} and *BCR-ABL*^{T315I} were expressed in the circulating hemocytes. The number of circulating hemocytes increased significantly in *BCR-ABL*^{P210} and *BCR-ABL*^{T315I} compared to the control. Moreover, the sessile hemocytes patterning was disrupted in both *BCR-ABL*^{P210} and *BCR-ABL*^{T315I}. In addition, melanotic tumors were observed in 30% of *BCR-ABL*^{T315I} expressing flies but not in *BCR-ABL*^{P210} flies. Upon examining the humoral arm of innate immune system in *D. melanogaster*, all three major pathways were dysregulated in *BCR-ABL*^{P210} and *BCR-ABL*^{T315I} expressing flies

Conclusions: We have established a *Drosophila* CML model to study the impact of expressing *BCR-ABL*^{P210} and *BCR-ABL*^{T315I} in the hematopoietic system. Future studies on this model can help decipher key genes/pathways involved in *BCR-ABL* mediated oncogenesis.

CONTENTS

	Page
ACKNOWLEDGEMENT	v
ABSTRACT	vi
LIST OF ILLUSTRATIONS	x
LIST OF TABLES	xi
Chapter	
I. INTRODUCTION	1
II. LITERATURE REVIEW	2
A. Chronic Myeloid Leukemia	2
1. Chronic Myeloid Leukemia Pathophysiology	2
2. BCR-ABL Aberrant Signaling	5
3. CML Treatment and Resistance	6
B. <i>Drosophila melanogaster</i> as a Model Organism	7
1. <i>Drosophila melanogaster</i> as a Model Organism	7
2. <i>Drosophila melanogaster</i> Hematopoiesis	8
a. <i>Drosophila melanogaster</i> Hematopoietic System	8
b. The Three Waves of Hematopoiesis and their Governing Signaling Pathways	11
i. Embryonic Hematopoiesis	11
ii. Larval and Adult Hematopoiesis	12
c. Sessile and Circulating Hemocytes	14
3. <i>Drosophila melanogaster</i> Innate Immunity	15
a. Cellular Immunity and Melanization	16
b. Humoral Immunity	18
C. <i>Drosophila melanogaster</i> and Hematological Malignancies	19

1. Mediators of Hematopoiesis and Tumorigenesis in Vertebrates and <i>D. melanogaster</i>	19
III. MATERIALS AND METHODS	23
A. Fly Stocks	23
B. The GAL4-UAS System	23
C. Imaging of Sessile Patterning and Melanotic Tumors	25
D. Hemocyte Count and Flow Cytometry	26
1. Hemocyte Count	26
a. Hemocyte Count Procedure	26
b. Hemocyte Count Calculation	27
2. Flow cytometry to determine GFP Hemocyte in Larval Bleed	28
E. Larval Bleed, Immunofluorescence and Confocal Microscopy Imaging ...	29
F. Assessment of Innate Immune Pathways Regulation through Expression of Antimicrobial Peptides	30
1. RNA Extraction	30
2. cDNA Synthesis	31
3. Real-Time Polymerase Chain Reaction (Real Time PCR)	32
4. Relative Gene Expression Analysis	33
5. Statistical Analysis	33
IV. RESULTS	34
A. Validation of <i>BCR-ABL</i> ^{P210} and <i>BCR-ABL</i> ^{T3151} Expression in Third- Instar Larval Hemocytes	34
B. <i>BCR-ABL</i> ^{P210} and <i>BCR-ABL</i> ^{T3151} Expressing Flies Have Increase in Circulating Hemocyte Number	34
C. <i>BCR-ABL</i> ^{P210} and <i>BCR-ABL</i> ^{T3151} Expressing Flies Show an Increase in GFP Positive Hemocytes by Flow Cytometry	35
D. Disruption of Sessile Patterning in <i>BCR-ABL</i> ^{P210} and <i>BCR ABL</i> ^{T3151} Expressing Larvae	35
E. Appearance of Melanotic Tumors in <i>BCR-ABL</i> ^{T3151} but not in <i>BCR ABL</i> ^{P210} Expressing Larvae	36

F. Assessing Humoral Immune Pathway Status in <i>BCR-ABL</i> ^{P210} and <i>BCR-ABL</i> ^{T3151} Expressing Larvae	36
V. DISCUSSION	46
A. Limitations and Future Perspectives	50
B. Conclusion	51
BIBLIOGRAPHY	53

ILLUSTRATIONS

Figure	Page
1: A schematic representation of the Philadelphia chromosome producing the t9:22 translocation.....	3
2: A schematic representation of BCR-ABL fusion protein isoforms and their association with various leukemias	4
3: A schematic showing the components of <i>Drosophila melanogaster</i> hematopoietic system	10
4: A schematic depicting the GAL4-UAS tissue targeting expression system	25
5: A schematic depicting a hemocytometer	27
6: Immunofluorescence staining of larval bleed	38
7: Hemocyte count in <i>BCR-ABL</i> ^{P210} and <i>BCR-ABL</i> ^{T3151} expressing larval bleed	39
8: GFP positive hemocyte population in larval bleed expressing <i>BCR-ABL</i> ^{P210} and <i>BCR-ABL</i> ^{T3151}	40
9: Disruption in sessile patterning in <i>BCR-ABL</i> ^{P210} and <i>BCR-ABL</i> ^{T3151} flies	41
10: Melanotic tumors in <i>BCR-ABL</i> ^{T3151} expressing 3 rd instar larvae	42
11: <i>Drosomydin</i> relative expression normalized to <i>RPL11</i>	43
12: <i>Diptericin</i> relative expression normalized to <i>RPL11</i>	44
13: <i>Tot A</i> relative expression normalized to <i>RPL11</i>	45

TABLES

Table	Page
1: Fly Strains used throughout the research project	24
2: Sequence and annealing temperatures for PCR primers	32

CHAPTER I

INTRODUCTION

Chronic Myeloid Leukemia (CML) is a myeloproliferative disease occurring in hematopoietic stem cells (HSC). CML results from a chromosomal translocation occurring between *Abelson (ABL)* gene and the *Breakpoint Cluster Region (BCR)* gene forming the Philadelphia Chromosome harboring the *BCR-ABL* oncogene which codes for a constitutively active tyrosine kinase. Several treatment modalities that target BCR-ABL tyrosine kinase, such as tyrosine kinase inhibitors (TKIs) have been proposed. However, mutations such as threonine substitution with isoleucine (T315I) are resistant to most TKIs. In addition, leukemic stem cells (LSC), which cause relapse in CML patients, are also resistant to TKIs. Thus, it is crucial to establish a model that would allow to decipher the signaling pathways which mediate this resistance and allow for screening of potential therapeutic drugs. Our group, created a *BCR-ABL*^{P210} and a *BCR-ABL*^{T315I} expressing transgenic fly line and validated it as a drug screening model through expressing a *BCR-ABL* in *D. melanogaster* eyes. This research project set the stepping stone for establishing a CML hematopoietic model in *D. melanogaster* for further genetic and drug screening. In specific, the aims of this research project were to:

- 1- Assess the effect of expressing oncogenic *BCR-ABL* (both wild type and T315I mutated form) on cellular immune responses mediated by hemocytes.
- 2- Assess the effect of expressing oncogenic *BCR-ABL* (both wild type and T315I mutated form) on systemic humoral immune responses.

CHAPTER II

LITERATURE REVIEW

A. Chronic Myeloid Leukemia

1. Chronic Myeloid Leukemia Pathophysiology

Chronic Myeloid Leukemia (CML) is a myeloproliferative neoplasm (1). The causative agent of CML; namely the Philadelphia chromosome was first described in 1960 by Nowell and Hungerford who observed the presence of a minute chromosome in the cells of CML patients (2). The Philadelphia chromosome is a result of a reciprocal translocation between *Abelson* murine leukemia gene (*ABL*) on chromosome 9 and *Breakpoint Cluster Region* gene (*BCR*) on chromosome 22 (3). This translocation creates the *BCR-ABL* oncogene which codes for the BCR-ABL fusion protein; a constitutively active tyrosine kinase (4) (Figure 1). Three forms of the *BCR-ABL* oncogene exists that can generate three different proteins of variable molecular weight; 190, 210 and 230 KD proteins depending on the breakpoint location on the *BCR* gene. All three forms will have similar portion of the *Abelson* gene (5). However, the BCR sequence is different among the three isoforms; in almost all CML patients and in one third of Acute Lymphoblastic Leukemia (ALL) patients, the breakpoint occurs in the major breakpoint cluster region coding for a p210 BCR-ABL fusion protein. The breakpoint may occur upstream in minor and translate into a 190 KD protein that is found in two thirds of the ALL patients and rarely in the Acute Myeloid Leukemia and CML patients (5)(6). Finally, the breakpoint can occur further

downstream producing a p230 fusion protein found most commonly in Chronic Neutrophilic Leukemia (CNL) patients (5) (Figure 2).

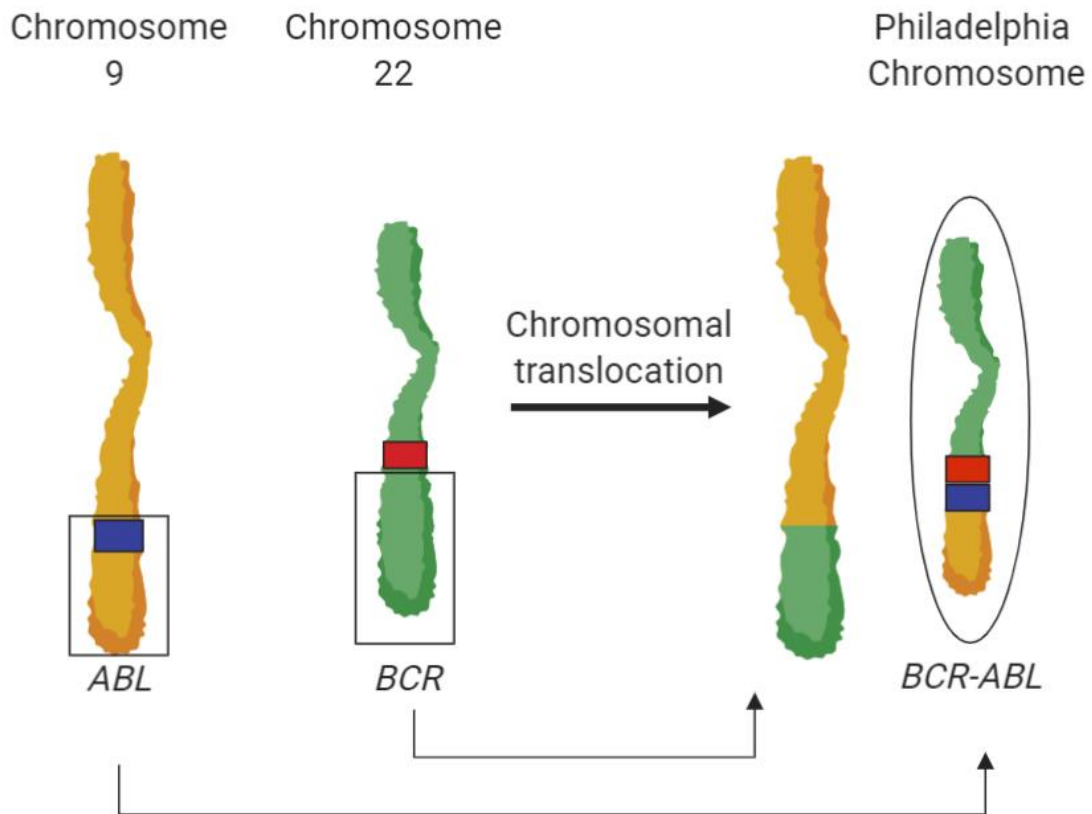


Figure 1: A schematic representation of the Philadelphia chromosome producing the t9;22 translocation. The chromosomal translocation between *ABL* gene on chromosome number 9 and *BCR* gene on chromosome number 22 which results in Philadelphia chromosome harboring the *BCR-ABL* oncogene which codes for a constitutively active tyrosine kinase. Schematic was produced by using Biorender.

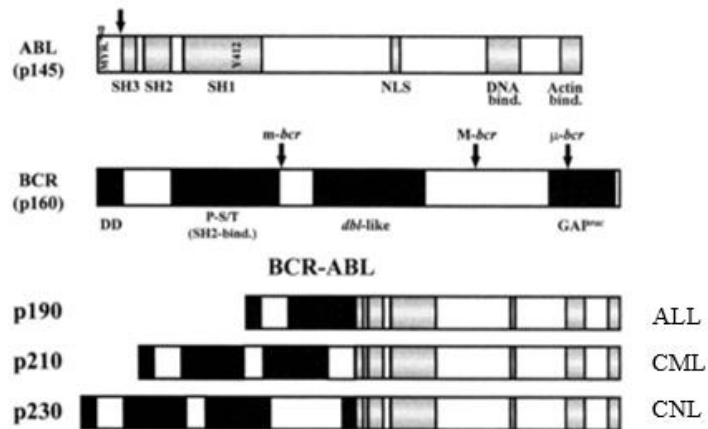


Figure 2: A schematic representation of BCR-ABL fusion protein isoforms and their association with various leukemias. The difference between the three proteins arise from the input of BCR rather than the ABL. The arrows on BCR protein show the location of protein fusion arising from three locations, namely m-bcr, M-bcr, and μ -bcr breakpoints which code for the p190, p210 and p230 respectively. Modified from Melo et al. ,1996 (5).

CML can be divided into 3 phases: chronic phase (CP), accelerated phase (AP) and blast crisis phase (BC). The early stage of the disease, in which 90% of the patients are diagnosed, is known as the chronic phase (7, 8). The CML-CP occurs because a hematopoietic stem cell gains the *BCR-ABL* oncogene that leads to proliferative advantage, expanding the myeloid compartment. In lack of any appropriate treatment, CML-CP can progress into an advanced stage; which is the accelerated phase followed by a blast crisis phase (7).

2. BCR-ABL Aberrant Signaling

The ABL protein normally shuttles between the nucleus and the cytoplasm. Upon fusion with BCR, the ABL protein becomes constrained in the cytoplasm. (6, 9). This retainment increases the interaction of the BCR-ABL with other cytoplasmic proteins and subsequently cause hyperproliferation, decreased apoptosis and disrupted transcriptional activity due to dysregulated Ras-mitogen-activated protein kinase (MAPK), phosphoinositide 3-kinase/AKT (PI3K/AKT) and Janus-activated kinase/Signal Transducer and activator of transcription (JAK-STAT) pathway and other pro-oncogenic pathways. (10).

The key post-translational modification required for BCR-ABL leukemogenesis is the phosphorylation of the 177th tyrosine residue on the BCR amino terminal (11). The phosphorylation allows the binding of the BCR to the SH2 domain of GRB2 adaptor protein. Son of Sevenless (SOS) protein attaches to the SH3 domain of the BCR-ABL/GRB2 complex (6, 12). This triple protein complex, BCR-ABL/GRB2/SOS, activates the downstream RAS pathway by converting the inactive GDP to active GTP on the RAS molecule. This constitutive activation of the RAS pathway, activates the MAP extracellular signal-regulated kinase (ERK) and the MAPK proteins stimulating abnormal cell proliferation (13).

Second, the BCR-ABL/GRB2/SOS complex activates the PI3K/AKT pathway through the activation of the RAS pathway (14) . The PI3K/AKT pathway promotes cell proliferation by activating mTOR, blocking autophagy, and suppressing the transcription factor forkhead O (FOXO). The PI3K/AKT pathway results in the phosphorylation of

multiple proteins that regulate the apoptosis process including Ask1, caspase 9 and MDM2, promoting the expansion of leukemic cells (15).

Moreover, the increased phosphotyrosine residues on BCR-ABL allows for the JAK-independent constant activation of STAT5 by binding to its SH2 domain. Normally, the STAT5 translocates to the nucleus with help of the receptor-associated JAK kinases which are activated following cytokine attachment to the receptors (16). The constitutively active STAT5, provides resistance against programmed cell death by downregulating molecules such as BAD, promoting apoptosis and upregulating molecules such as BCL-xL that inhibits apoptosis (10).

All these pathways activated by BCR-ABL indicate that its transforming ability lies in its constitutively active tyrosine kinase activity.

3. CML Treatment and Resistance

The first drug to be released that would directly inhibit the tyrosine kinase activity of BCR-ABL was Imatinib. It is the first choice given to patients who are in early chronic phase upon diagnosis (17). Imatinib provided good cumulative complete cytogenetic response (CCyR) and high survival rates (18). However, some patients do not respond well to Imatinib and would have poor long-term prognosis with increased chances of later recurrence (19). The need for drugs that would overcome Imatinib resistance led to the development of second-generation tyrosine kinase inhibitors, such as Dasatinib and Nilotinib. Dasatinib inhibits both BCR-ABL, Src, platelet-derived growth factor and other kinases, acting as a less-selective drug compared to Nilotinib (20). Nevertheless, both

Dasatinib and Nilotinib showed greater CCyR and major molecular response compared to Imatinib and in cases of Imatinib resistance opening the possibility of second-generation TKIs being used as a first-line treatment (20).

Despite the advancement offered by the second-generation TKI, there are certain cases of BCR-ABL mutant leukemic clones where these drugs are completely ineffective. One of these mutations, referred to as the Achilles heel, is the T315I mutation resulting from the substitution of threonine with isoleucine at the 315th position of ABL (21). This mutation removes a hydrogen bond in ATP-binding pocket where first and second-generation TKI would normally attach and exert their inhibitory effect (22). Several drugs in development have been proposed for the BCR-ABL^{T315I} clones such as Rebastinib and AT9283 to inhibit the mutation which accounts for relapse in one out of five cases of CML (25). One TKI that showed efficacy against the gate keeper T315I kinase mutation is Ponatinib which works against BCR-ABL and other kinases such as PDGFR- α (23, 24). However, due to its pan-activity on different kinases, severe side effects and high toxicity, it has been suspended for a period and later given to patients with great precaution and several warnings (25).

B. *Drosophila melanogaster* as a Model Organism

***Drosophila melanogaster* as a Model Organism**

For the last century *D. melanogaster* has been used as a model organism in biomedical research. Using fruit flies offers many benefits compared to vertebrate models; they are easily reproducible in a laboratory setting, produce a big number of offspring in each

generation, have a short life cycle, and have wealth of genetic tools that can be used to address specific biological questions. These advantages allowed for the extensive study of various developmental, neurobiological, behavioral and genetic processes in fruit flies (27). Although, *D. melanogaster* and humans may be phenotypically dissimilar, the fundamental developmental and genetic processes have been evolutionary conserved between the two species (28). Additionally; in recent years *D. melanogaster* has been increasingly utilized to model hematopoietic diseases and malignancies. This is due to similar molecular mechanisms and pathways regulating hematopoiesis and blood cell development in both *D. melanogaster* and vertebrates.

1. Drosophila melanogaster Hematopoiesis

a. *Drosophila melanogaster* Hematopoietic System

Like vertebrates, *D. melanogaster* contains a progenitor cell type that expresses different markers as it matures over time. Its hematopoietic system supports a cell of stem-like or multipotent nature, which through its communication with the hematopoietic niche maintains its stem cell properties. Moreover, the *D. melanogaster* hemopoietic organ during the larval stage, the lymph gland, develops under the control of certain signaling pathways that are homologous to those that control the mammalian aorta-gonad mesonephros in mammals.

The *D. melanogaster* hemolymph contains three types of cells: the plasmatocytes, the crystal cells and the lamellocytes (Figure 3). Plasmatocytes account for 95% of the total hemocytes population in a healthy fly (29) (Figure 3). They are macrophage-like cells that can phagocytose bacteria and apoptotic debris (30). They also can secrete cytokines-like

molecules as well as antimicrobial peptides aggravating an already established humoral immune response (30, 31).

Several receptors help plasmatocytes identify their targets for phagocytosis. For example, the peptidoglycan recognition protein is one of the receptors involved in the recognition of microbial pathogens. Other receptors are involved in the recognition of apoptotic bodies such as Draper (32), Phosphatidyl serine receptor (PSR) (33) and Croquemort (Crq) (34). On the other hand, receptors such as Dscam, Nimrod and Eater mediate the phagocytosis of bacteria (35-37).

The remainder hemocytes are crystal cells which, as their name suggests, contain para-crystalline structures composed of prophenoloxidase (PPO) which is a key member in the melanization process that crystal cells perform (38). This process is homologous to wound healing in mammalian system and is mediated by the conversion of phenols to oxidase by an enzyme called phenoloxidase (PO). This conversion results in the deposition of melanin that causes a darkening of tissue under the epithelia. PPO is cleaved into its active form of PO following the activation of a serine protease signaling cascade (39-41). Although PPO can be found throughout the hemolymph, the PO activity is controlled where it only occurs in a wound site upon crystal cell rupture (42). The clot that is formed by the coagulation of the hemolymph is aided by the disposition of melanin at that site causing the hardening of the clot and the closure of the wound site.

Finally, the lamellocytes which are the largest of the hemocytes in size exist in very low numbers if not at all during *D. melanogaster* normal life cycle. Their differentiation is stimulated upon the parasitization of the fruit fly, sterile wounding or once

a foreign body accesses the hemocoel through an injection (43). The main function of these cells is the encapsulation of foreign material that cannot be removed by phagocytosis; during which they work hand-in-hand with plasmatocytes and can collaborate with crystal cells during the melanization process (44).

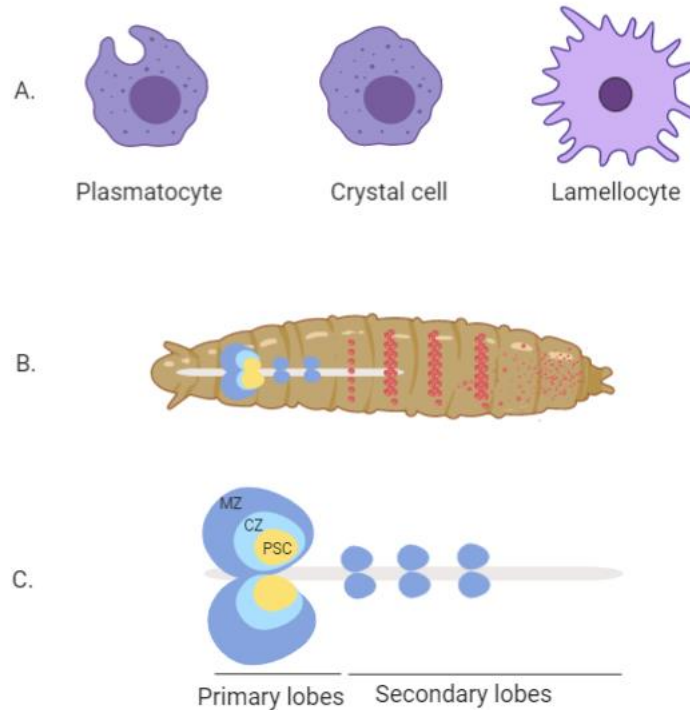


Figure 3. A schematic showing the components of *Drosophila melanogaster* hematopoietic system. (A) depicts the three types of circulating hemocytes found in the fruit fly hemolymph. (B) shows the lymph gland and the sessile hemocytes found during the larval stage of *D. melanogaster* (red cells). (C) represent the lymph gland primary and secondary lobes as well as the three zones of the primary lobes, the medullary zone (MZ), the cortical zone (CZ) and the posterior signaling center (PSC). Schematic was produced using Biorender

b. The Three Waves of Hematopoiesis and Their Governing Signaling Pathways

In vertebrates, hematopoiesis occurs over two waves that are distinct in their location within the organism (45-47). The primitive phase that occurs in the embryonic yolk sac produces the erythroid cell. On the other hand, the definitive phase occurs later during development and starts de novo in the aorta gonad mesonephros (AGM) (46).

In *D. melanogaster* there are three waves of hematopoiesis, the primitive, definitive and later the adult hematopoietic-hub phase over which the specification of different sets of hematopoietic precursors occur. First, the primitive phase occurs in the head procephalic mesoderm where around 800 cells become specified, move through the developing embryo and are part of the hemocytes in the circulation later in the larval stage (48). The definitive hematopoiesis occurs at a later stage during embryonic development, in the cardiogenic mesoderm, where a set of hemopoietic precursors are specified to later form the lymph gland (49, 50). The lymph gland provides most of the cells in the circulation in the adult fly upon its disintegration at the onset of metamorphosis releasing mature blood cells into the circulation (51).

i. Embryonic Hematopoiesis

In the primitive wave of hematopoiesis, 800 cells differentiate (48, 49). Most of these *Serpent* (*Srp*) expressing cells are plasmatocytes that migrate through the embryo, or crystal cells that are localized in the head region (46, 52-55). The later interaction with transcription factors will determine the cell fate. The Glial cell missing (*Gcm 1* and *Gcm 2*) transcription factors determine the cell fate of plasmatocytes (56). However, *Gcm* is

downregulated in the anterior region of the head primordium to allow for the expression of the *lozenge*. *Lozenge* interacts with *Srp* to determine crystal cell fate (46, 57). The *D. melanogaster* Platelet derived growth factor/ Vascular endothelial growth factor (PDGF/VEGF) otherwise known as, PVR, is homologous to the VEGF receptor signaling pathways in mammals. In *D. melanogaster*, three PVR ligands are present in the embryonic head mesoderm helping plasmatocytes dispersal throughout the embryo. This indicates that PVR signaling pathway in *D. melanogaster* functions to direct plasmatocytes migration (55, 58).

ii. Larval and Adult Hematopoiesis

The lymph gland is located approximately one third of the larval length from the anterior end towards the dorsal side beneath the brain (59). It develops from a set of cell cluster that arises from the cardiogenic mesoderm along with the heart-like tube, the dorsal vessel as well as nephrocyte- like pericardial cells (49, 50). A single precursor cell in the cardiogenic mesoderm gives rise to the dorsal vessel and lymph gland (60). This resembles the mammalian hemangioblast, which can develop into both the blood and vascular cells (5,6).

The lymph gland consists of a pair of primary lobes located anteriorly and several posterior lobes. The primary lobes can be further divided into several zones, the medullary zone (MZ), the cortical zone (CZ) and the posterior signaling center (PSC) (Figure 3). The different lobes develop sequentially during the *Drosophila* life cycle with the primary lobes developing prior to the posterior lobes. During the 12th to the 16th stage of embryogenesis, three clusters of 20 cells located between the thoracic segment T1-T3 and surrounding the

dorsal vessel, fuse together(60). These clusters expand actively to 200 cells during the second -instar larval stage and further to 2000 cells during the third- instar larval stage. These cells will establish the lymph gland anterior-most lobes; the primary lobes (50). The secondary lobes appear later during the second-instar larval stage (61).

It is not until the late-second to early third instar larval stage that the lymph gland appears as distinct organ with the primary lobes discernable as specific structures containing variable zones. Located towards the periphery of the primary lobe is the CZ which appears as a collection of cells that are loosely packed and granular in appearance. On the contrary, the cells towards the center of the primary lobe forming the MZ are compact in organization. The third zone, the PSC constitute 50 cells during the third-instar stage but is not structurally distinctive. In addition to the architectural variation, each zone expresses its own collection of markers which is indicative of the nature of the residing hematopoietic population (50). For example, the medullary zone, supporting hematopoietic progenitor cells, expresses E-cadherin (31), Domeless (62) and Unpaired (31) which are pro-hemocyte markers. While the cortical zone expresses mature hemocyte markers such as Hemolectin (63), Peroxidase (64) and Lozenge. On the other hand, the PSC expresses a set of markers such as Antennapedia (65) and Collier (66). The PSC mediates signaling pathways such as the JAK/STAT and hedgehog to maintain the progenitor state of the hemocytes in the medullary zone (65, 67). It is also the site for lamellocyte differentiation (66).

Posterior to the primary lobes are three bilateral lobes known as the posterior lobes. They express a set of markers similar to that of the medullary zone such as Domeless and

E-cadherin suggesting they support hematopoietic progenitors. However, contrary to the cells of the medullary zone that quiesce during the third instar stage, the cells of the secondary lobes continue proliferating similar to the cells in the cortical zone. This suggests that the pro-hemocyte population in the secondary lobes is different from the population in the medullary zone (50). Under normal conditions the proliferating cells of the posterior lobes do not fully differentiate and thus express a subset of differentiated hemocytes markers (68). The cells rather enter circulation and a portion of them form the adult hematopoietic hubs acting as the adult hematopoietic niche and attach to the drosophila body wall (69). These proliferating pro-hemocyte cells only differentiate from their progenitor stage upon the presence of an immune-stressor (50, 61) .

c. Sessile and Circulating Hemocytes

Following their production in the head mesoderm during embryogenesis, the hemocytes can end up as circulating or sessile hemocytes during the larval stages. The first group circulates in the hemolymph while the second group are attached to the larval body wall in distinct sessile groups located in epidermal-muscular pockets found between the epidermis and muscle layers of the larvae (70-72) (Figure 3). The sessile hemocytes form lateral patches that later produce distinct dorsal stripes. Several pathways mediate the homing of hemocytes to the sessile pools. For example, Jun N-terminal kinase (JNK, Basket), Rac1 GTPase and Eater transmembrane receptor ensure adhesion and homing of the hemocytes following the innervation of peripheral nerves. The innervation of the peripheral nerves facilitates the proliferation and adhesion of hemocytes through transforming growth factor (TGF- β) signals (72-74). The sessile hemocytes are isolated from the hemolymph and

independently regulated from the circulating hemocytes, however, the sessile pool can exchange cells with the circulating hemocyte population. The complete release of sessile hemocyte from their pool into the hemolymph would require physical disruption to the larva compared to the circulating hemocytes that upon puncture of the cuticle would be released in the hemolymph bleed (72). Through Notch signaling, mature plasmatocytes in the sessile bands can transdifferentiate into crystal cells (75). In addition, mature plasmatocytes in the sessile pockets can transdifferentiate into lamellocytes after parasitization as well as the absence of U-shaped (76, 77). A wasp infection or an immune stressor can cause the transdifferentiation of both circulating and sessile hemocytes into lamellocytes through disruption of Wnt/Wg signaling. This results in the increase of circulating hemocytes number due to the release of the lamellocytes from the sessile pools (76). The continuous activation of Toll immune pathway can also disrupt sessile hemocytes pools as seen in Toll^{10b} mutants (78). A very important note is that circulating hemocytes do not proliferate themselves. The release of sessile cells from their compartments or differentiation of the hemocytes found in the prohemocyte pool in the lymph gland is what can contribute to an increase in the number of circulating hemocytes (72, 79).

2. *Drosophila melanogaster* Innate Immunity

D. melanogaster is devoid of adaptive immunity and thus rely heavily on innate immunity to recognize and protect itself against the various pathogens it encounters in nature. This feature has promoted *D. melanogaster* to be an excellent model to extensively study the intricacies of the innate system reactions that would otherwise be concealed by the adaptive immune system. The first reaction is one provided by the epithelial barrier; whether it is the

cuticle surrounding the organism or the epithelial tissue surrounding internal organs such as the trachea or the gut. Second, there is the cellular immune response provided by the blood cells that perform an array of functions such as; phagocytosis of foreign bodies, melanization and coagulation as a form of wound healing in addition to the encapsulation of parasites. Finally, the fat body - analogous to mammalian liver - can provide humoral immunity by producing antimicrobial peptides against bacteria and fungi through producing the majority of anti-microbial peptides. Even though each pathway is activated by specific microbes, the immune pathways can cooperate to activate a greater range of genes downstream of the pathways in case of certain parasitic infections.

a. Cellular Immunity and Melanization

Hemocytes in *D. melanogaster* are one of the primary lines of defenses due to their speed in sensing stress and mitigating it compared to systemic immunity provided by the AMP of the fat body (80). According to Banerjee et al., the stress can be attributed to several factors that can disrupt homeostasis whether intrinsic arising from genetic mutations and tissue growth or rather extrinsic stemming from parasitization, injury or microbial infection (81).

Genetic mutations can produce tissue abnormality that imposes an internal stress on *D. melanogaster*. For example, several *D. melanogaster* models introduce mutations which disrupt the basement membrane, disturb cell polarity markers and cause loss of proper cell-to cell contact. Such mutations disrupt the extracellular matrix that intricately separate the hemolymph from the tissue and result in “auto-immune” hemocyte responses (82). These responses include; the adherence of the plasmatocytes to the affected tissue followed by the activation of hemocyte differentiation pathways and the formation of

melanotic tumors by lamellocytes to encapsulate the disrupted self-tissue (82-84). A paper by Pastor-Pareja, has discussed how disruption of basement membrane in a metastatic tumor model expressed in the eye discs limited tumor growth through the induced proliferation of plasmatocytes and their recruitment to the disrupted tissue (83). Another example of genetic mutations is in *D. melanogaster* leukemia models where mutations affect hemocytes proliferation and differentiation. In fly leukemia models, human oncogenes are expressed in the hematopoietic system and result in the upregulation of circulating hemocyte numbers, preferential differentiation of lamellocytes and the surrounding of normal tissue by melanotic tumors (85-87). Similar phenotypes, such as upregulation in lymph gland proliferation and subsequently its hypertrophy, in addition to formation of melanotic tumors around normal tissue occurred in the case of mutant flies that result in overactivation of JAK/STAT and Toll pathways (88-90).

In general, melanotic tumors can be divided into two classes. Class I melanotic tumors encapsulate abnormal self-tissue that has undergone basement membrane disruption through knockdown of ECM protein. In this case, the *D. melanogaster* cellular immunity is functioning normally (84). However, Class II melanotic tumors develop upon augmented or overactive immune system which results in hemocyte activation and abnormal melanization of normal healthy tissue. Class II melanotic tumors are often accompanied by a higher number of circulating blood cells, disruption of Toll, JAK/STAT and adenosine signaling (88-91). For example, in one paper where human oncogene *AML1-ETO* was expressed in *D. melanogaster* hemocytes, melanotic tumor resembling Class II melanotic tumors were formed (89). Thus melanotic tumors provide easy way to identify phenotypes in large

genetic screen studies since it is correlated with disruptions of normal proliferation and differentiation of cells and hemocytes (81).

b. Humoral Immunity

D. melanogaster can discriminate between pathogens based on the surface molecules they possess. Based on this information, either one of the NF- κ B transcription factors can be activated, Dorsal/Dif or Relish representative of the Toll or IMD pathway respectively.

The Toll pathway is responsible for providing protection for the fly against fungal and gram-positive bacteria. It is also responsible for directing the dorsal-ventral polarity of cells in a *D. melanogaster* embryo (92). First discovered in *D. melanogaster*, the Toll receptor in flies does not bind directly to the pathogen like its vertebrate counterpart. The transmembrane Toll 1 receptor in flies is activated by a processed homologue of the nerve growth factor, Spätzle. Once the Toll pathway is activated, the intracellular MyD88, Pelle kinase and Tube causes the degradation of a triple complex composed of NF- κ B protein Dorsal/Dif and I κ B protein Cactus. Cactus is then broken down and Dorsal and Dif localize to the nucleus where they activate *drosomycin* and *metchnikowin* (93, 94). The toll pathway is an important regulator of hemocyte number in the hemolymph and their proliferation in the lymph gland (88, 95).

IMD pathway on the other hand protects the fly from Gram-negative bacterial infection and is mainly involved in immunity compared to the toll pathway (96). The bacterial component directly attaches to the peptidoglycan recognition protein-LC receptor. This attachment activates a sequence of downstream proteins such as TAB2 AND TAK1 which act on a IKK complex composed of two proteins IKK β and IKK γ that phosphorylates

Relish. The NF- κ B protein Relish has an inhibitory domain and a Rel domain. Once Relish is phosphorylated, it is cleaved by Dredd and the Rel domain localizes to the nucleus where it activates a series of genes such as *dipetricin*, *definsin*, *attacin*, and *cepronins*. Although the activating pathogens, inhibitory regulators and timeline of activation following injury are different, some antimicrobial peptides (AMP) products can be dually activated by both pathways (97). Importantly, in a paper that used three *Drosophila* leukemia models which harbored oncogenes with concurrent depletion of tumor suppressor genes both IMD and Toll pathway were dysregulated (98).

JAK/STAT pathway provides defense from viral infection and like the toll pathway is involved in development. The pathogen specific molecules and the activation of the pattern recognition receptor (PRR) in the JAK/STAT pathway are not clearly understood. However, the downstream protein Domeless activates the transcription factors Hopscotch and STAT92E which will consequently activate the expression of immune and stress-responsive genes such as *Tep1* and *Tot A* (99, 100).

***C. Drosophila melanogaster* and Hematological Malignancies**

1. Mediators of Hematopoiesis and Tumorigenesis in Vertebrates and *D. melanogaster*

Mammalian hematopoietic stem cells rely on cues from its microenvironment, the HSC niche, to self-renew and differentiate into various blood cells (101). Disruption in the HSC and niche signaling results in leukemias such as AML (102). The simplicity of the *D. melanogaster* hematopoietic niche, the PSC, and its hematopoietic system provides a reductionist model to guide the understanding of the genetic and cellular signaling between the HSC and its niche hematopoietic system and the underlying factors behind

transformation in hematological malignancies. In vertebrates, JAK/STAT, Hedgehog, Wnt, JNK signaling regulate immature HSC state and thus are key players in hematological malignancies. Several studies have looked at the impact of these signaling pathways on *D. melanogaster* hematopoiesis. For example, in human leukemia one of the contributing factors is a constitutive activation of mutated JAK/STAT (103). Specifically, a mutation of human JAK2 has been implicated in the pathogenesis of various forms of AML (104). Similarly, overexpression of mutated JAK gene *hop^{Tum-1}* results in the formation of melanotic tumors in the lymph gland and proliferation of prohemocytes in fruit fly (90). In addition, overexpression of STAT transcription factor (STAT92E) in *D. melanogaster* induced tumorigenesis in the fly adult eye and formation of melanotic tumors in the larval stage (105). On the other hand, Notch signaling which is vital in the commitment of the lymphoid cells is required for preservation of the PSC cell identity in the *D. melanogaster* Lymph gland through controlling the levels of Col transcription (106, 107). Activation of Notch signaling is also needed to determine crystal cell differentiation (108). Sima, the *D. melanogaster* orthologue of Hypoxia inducible factor- is required to activate Notch receptor and commit prohemocyte to a crystal cell fate (109). In vertebrates, Wnt signaling has been implicated in HSC homeostasis and niche maintenance to promote self-renewal of HSC. Likewise, Wnt signaling in the fruit fly results in the favoring proliferation of prohemocytes over differentiation by inhibiting the PSC (86, 110). In addition, FOXO and JNK pathways can promote the premature differentiation of prohemocytes through increasing the level of reactive oxygen species (ROS) beyond their normal levels in hemocytes progenitors. This correlates with ROS species build up in mammals that occur in differentiating common myeloid progenitors as a result of oxidative stress (111, 112).

The previous studies strengthen the notion of *D. melanogaster* as a hematological malignancies model in hope to provide a therapeutic outlet through understanding the genetic and cellular mechanisms that mediate tumorigenesis.

In addition to dissecting the molecular signaling pathways that mediate the interaction between the HSC and the HSC niche, several studies used the fruit fly to model human leukemia directly in hematopoietic tissue. For example, a study by Sinenko et al., expressed *AML-1/ETO*, a chromosomal translocation that results in AML in the hemocyte lineage using the UAS/GAL4 system. The tissue-specific expression caused the expansion of the prohemocyte cell population in the lymph gland that resulted in the hyperproliferation of the circulating hemocytes (86, 113). The establishment of *D. melanogaster* AML model paved the way for performance of genetic screens to identify suppressors of the hyperproliferation of the hemocytes. As an example, Osman et al. identified calpain B through an RNAi genetic screen to be an important mediator of the *AML1-ETO* pathogenesis. Interestingly, calpain B was also shown to mediate *AML-ETO* pathogenesis in human leukemia cell lines (85). In addition, several papers have studied the impact of expressing Acute Lymphoblastic Leukemia (ALL) (114), AML (85, 86, 115-118), Human T-cell lymphotropic virus type 1 induced adult T cell leukemia (HTLV-1) (119) and CML (120) (121-123) oncogenes in the *D. melanogaster* hematopoietic system and subsequently observed transformative phenotypes, such as an increase in hemocyte number, disruption in lymph gland architecture and in certain cases of lethality. However, only one of the above studies looked at validating *D. melanogaster* as a drug screening model. The paper by Al Outa et al., expressed wild-type and mutated *BCR-ABL* and

validated its usage in a drug screening model through reversal of rough eye phenotype and lethality (123).

CHAPTER III

MATERIALS AND METHODS

A. Fly Stocks

Standard *Drosophila* husbandry protocols were followed to set crosses and create screening lines (Figure 4). Fly stocks used, their site of expression and Bloomington number are indicated in Table 1. Fly stocks were raised at 25°C while crosses were performed at 29°C. Virgin flies were easily identified through the presence of the meconium; a dark spot present in the ventral abdominal wall.

B. The GAL4-UAS System

The binary GAL4-UAS system relies on the GAL4 yeast protein that binds to the upstream activating sequence (UAS) and allows temperature dependent transgene expression. This binary system allowed the expression of *BCR-ABL* in targeted tissue through crossing a GAL4 driver strain to *UAS-BCR-ABL* responder strain indicated in Table 1. The GAL4 driver strain would harbor the transcription activator, the GAL4 downstream of the specific tissue promoter. The UAS responder strain would harbor the UAS upstream of the desired gene of interest. Upon crossing, the GAL4 would be expressed under the control of the tissue specific promoter. Consequently, the GAL4 protein binds to the UAS and drive the expression of the gene of interest in the desired tissue (125) (Figure 4). Throughout the study we used *Hml Δ-Gal4; UAS-GFP* driver which express GFP in all hemolectin expressing cells (differentiated hemocytes and lymph gland). The cross *Hml Δ-Gal4; UAS-GFP > w1118* were used as control, (expressing GFP protein in the differentiated

circulating hemocytes and the lymph gland cortical zone). *Hml Δ-Gal4; UAS-GFP > BCR-ABL^{P210}* and *Hml Δ-Gal4; UAS-GFP > BCR-ABL^{T315I}* express the *BCR-ABL* oncogene in differentiated hemocytes and lymph gland upon crossing them to each other. *UAS-BCR-ABL* has a Myc tag to follow expression of the transgene.

Table 1. Fly strains used in this study. The table indicates the site of expression and source for each strain.

Fly strain	Site of expression	Bloomington number
<i>w1118</i>	Wild type flies with white colored eyes used as a control strain.	BDSC: 3605
<i>Hml Δ-Gal4; UAS-GFP</i>	GAL4 driver strain that expresses GAL4 proteins under the control of <i>Hml</i> gene promoter allowing GAL4 and GFP protein expression in differentiated embryonic and larval hemocytes (plasmatocytes and crystal cells) + Lymph gland cortical zone (124)	BDSC: 30140
<i>UAS-BCR-ABL^{P210}</i>	UAS responder strain that controls the expression of the wildtype fusion oncogene <i>BCR-ABL</i> .	(Al Outa et al., 2019)(123)
<i>UAS-BCR-ABL^{T315I}</i>	UAS responder strain that controls the expression of a fusion oncogene <i>BCR-ABL</i> carrying a T315I mutation in the ABL domain.	(Al Outa et al., 2019) (123)

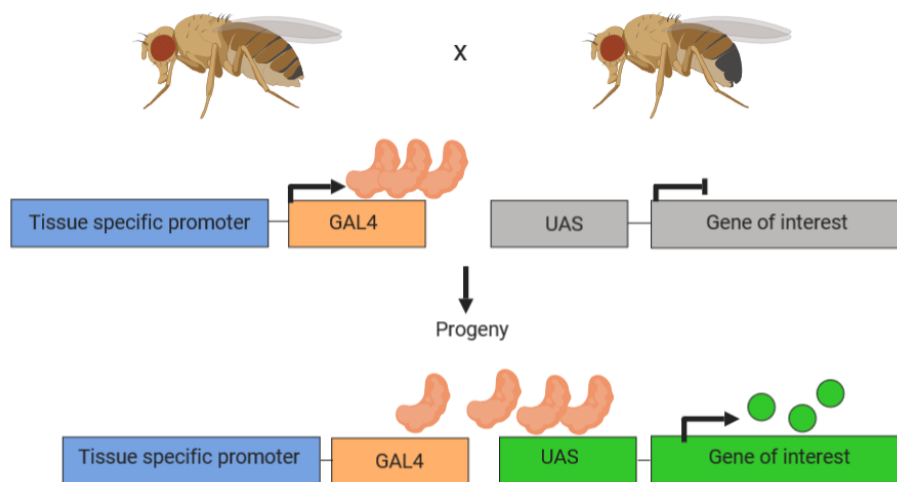


Figure 4. A Schematic depicting the GAL4-UAS expression system. One fly harboring the GAL4 driver strain would be crossed to a fly harboring the responder strain. Following the crossing of the two strains, the tissue specific promoter allows the expression of the *GAL4* and the Gal4 protein binding to the UAS. Thus, promoting the expression of the gene of interest in the target tissue. The schematic was produced using Biorender.

C. Imaging of Sessile Patterning and Melanotic Tumors

Late wandering third-instar larvae were picked from the walls of the food vial with a pair of forceps and cleaned from food and debris by placing them in a 1X Phosphate Buffered Saline (PBS) (Sigma Aldrich, St. Louis, MO) filled petri plate before being transferred using forceps (Electron Microscopy Sciences, Dumont, Number 5, Hatfield, PA) to a tissue paper to dry them. Larvae are then placed in an Eppendorf in -80°C for one and a half minute. They can be left in the -20°C for 20 minutes or for 4 hours in the 4°C . However, it is at -80°C that the larvae show the sessile patterning best (79). The Eppendorf are then placed on a plate on ice. The larvae were then imaged for both sessile patterning and melanotic tumor distribution using an SZX2-ILLT GFP Olympus microscope (Olympus, Tokyo, Japan) while submerged in a drop of 100% glycerol (Sigma-Aldrich, St. Louis, MO) (Protocol modified from Anderl et al, 2016.)

D. Hemocyte Count and Flow Cytometry

1. Hemocyte Count

a. Hemocyte Count Procedure

Late wandering third-instar larvae were picked from the walls of the food vial with a pair of forceps and cleaned from food and debris by placing them in a 1X PBS filled petri plate before being transferred using forceps to a tissue paper to dry them. The larvae are kept in the petri plate on ice throughout the bleed process to minimize their movement. For the wild type larva bleed, 13 μ l of 1X-PBS is placed on parafilm strip under a light microscope before transferring the larvae into the PBS drop. For larva carrying the transgene, 40 μ l of 1X-PBS is placed on parafilm strip. Using two pair of forceps the larva is secured in place by the nondominant hand while the other pair of forceps is placed just beneath the cuticle and pushed to the outside to release the hemolymph on the parafilm strip. The hemolymph can be observed as viscous liquid in the parafilm strip. The larva is allowed to bleed for 30 seconds then using one side of the forceps the larva is removed not to lose a greater volume of the bleed. Throughout the bleed process it is best not to use a brush to avoid disrupting the sessile hemocytes and releasing them into the circulation. The hemolymph bleed is mixed thoroughly with a pipette before taking 10 μ l of the bleed and placing it in a Neubauer chamber (Buerker-Turk, Marienfeld, Germany) with a coverslip attached beforehand. The Neubauer chamber is placed under an Axiostar plus light microscope (Zeiss, Oberkochen, Germany) and number of cells in each of the four quadrant is noted down and the cells lying on two of the border lines in each quadrant (highlighted in red) were added to the cells found in each quadrant (Figure 5).

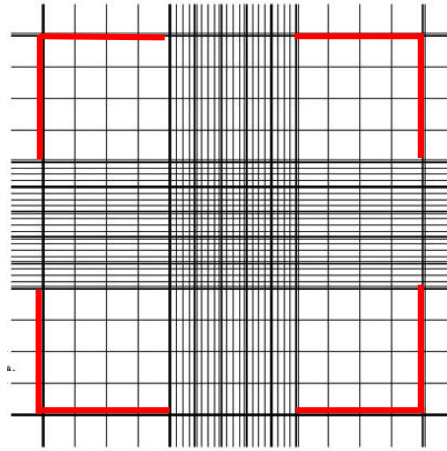


Figure 5. A schematic depicting a hemocytometer. The red lines indicate the border lines considered as part of the quadrant during hemocyte count.

b. Hemocyte Count Calculation

Hemocytes are reported as hemocyte count per milliliter of bleed or they can be reported as hemocytes/larvae. In the result section of the thesis work it is reported as hemocytes per milliliter bleed. Each square in a hemocytometer with a coverslip placed properly represents 10^{-4} cm^3 . Each 1 ml is equivalent to 1 cm^3 , thus;

$$\text{Cells per ml} = \text{Average number of hemocytes in all 4 quadrants} \times \text{Dilution factor} \times 10^4$$

with $\frac{Q1+Q2+Q3+Q4}{4} = \text{Average Hemocyte number in four quadrants}$

4

For example, if one larva is initially bled in 40 μl and only 10 μl are taken in a Neubauer chamber the dilution factor is then 4. For the wild type the dilution factor is 1.3.

2. Flow Cytometry to Determine GFP Positive Hemocytes in Larval Bleed.

For the bleed, 8% BSA- 1x PBS solution is prepared. BSA (Bovine Serum Albumin, Sigma Aldrich) should be well mixed with PBS. On a Parafilm strip 5 larvae are placed in a 40ul drop of 8% BSA- 1XPBS and bled by pricking their cuticle using a pair of forceps. The larvae are allowed to bleed for 30 seconds before removing the bleed and suspending it in 160ul of 8%BSA- 1X PBS in a 0.65ml Eppendorf. Same procedure is done for w1118 to be taken as negative control (79). The flies are freshly bled and taken to the Guava Millipore machine (Guava EasyCyte8 Flow Cytometer-Millipore, Merck/Sigma, Burlington, MA). The events are set to 10000 as it allows for easier observation of changes in GFP positive cells count. The sample is vortexed before it is run. The w1118 flies bleed is run first and the GFP fluorescence signal threshold is set so that it does not exceed 10^1 . Any cells with fluorescence below 10^1 are included in the non-GFP population while cells with higher fluorescence were considered GFP positive. The Gain controls are set to 378 for the Forward scatter, 159 for the Side scatter and 8 for the green fluorescence. These controls allowed for the best distribution of events across the plot. Each sample was repeated 3 times and each Eppendorf contained a pooled bleed of 5 adults. Following runs the plots are gated with two gates; GFP and non-GFP populations, with each gate encompassing the cell count, percentage and mean. The percentage of GFP cells in each sample was noted and plotted in a graph. Protocol was adapted from Anderl et al., 2016 (79).

F. Larval Bleed, Immunofluorescence and Confocal Microscopy Imaging

Following the same protocol as hemocyte bleed, late wandering third-instar were bled in 10 μ l of 1X-PBS in a 12 well plate. The slides with the bleed are placed in a humidified chamber for 30 minutes at 25 °C for the cells to adhere. The humidified chamber is created by covering a box with wet tissue and parafilm. The PBS is removed, and 4% formaldehyde (Sigma-Aldrich, St. Louis, MO) is added for 30 minutes to fix the cells. Formaldehyde is removed, and the cells are washed with 1X PBS- 0.3% Triton (PBST) twice for 5 minutes each time. Then a blocking solution of 5% Normal Goat Serum (NGS) (Dako, Santa Clara, CA) dissolved in PBST is added to the cells and left for 10 minutes. Following the blocking stage, primary antibody is added to the samples in (1:50 concentration) dissolved in 5% NGS in PBST. The primary antibody used was anti-c-Myc-tag antibody, pAB, Rabbit (Genscript, Piscataway, NJ). The cells are left to incubate with the primary antibody overnight in a 4°C environment. The cells are then washed twice with PBST for 5 minutes. Then, Alexa-594 fluorochrome-conjugated anti-rabbit secondary (Abcam, Cambridge, UK) diluted in 1:500 concentration in 5% NGS PBST solution is added to the cells. The cells are then washed two times each for 5 minutes with 1X PBS. Then 5% DAPI solution is added for 5 minutes before adding Fluoroshield Mounting Medium with DAPI (Abcam) and securing a coverslip over the sample. The cells are then imaged using a laser scanning confocal microscope (laser scanning confocal microscope (Carl Zeiss Laser Scanning Microscopy 710, Jena, Germany). DAPI, EGFP and Alexa 594 lasers are used to picture the cells at 40X and 63X oil magnifications to confirm the co-localization of the MYC, GFP and DAPI signals in the same cells (Protocol modified from Evans et al., 2014 (124)).

G. Assessment of Innate Immune Pathways Regulation through The Expression of Antimicrobial Peptides

1. RNA Extraction

Total RNA is extracted using Trizol (TRI reagent, Sigma Aldrich) from 25 adult females in a 2ml eppendorf according to a protocol optimized in Shirinian's lab. Working under the fumehood, 150µl of Trizol is added to the adult flies. The flies are grinded using a pestle for 30 seconds intervals with 10 seconds break time to place eppendorf back on ice. After thorough grinding, the pestle is washed with additional 150 µl of Trizol. Then, the eppendorf is left to incubate for 5 minutes at room temperature under the fume hood. Afterwards, the fly eppendorf is spun at max speed at 4 °C for 5 minutes. Following the centrifugation, chloroform (Sigma-Aldrich) is added to the Trizol in a ratio of 1:5 (Chloroform: Trizol). Thus, for a total of 300 µl Trizol 60 µl of chloroform are added. The sample tube is then shaken very well until a pink turbid liquid forms. Afterwards, the sample tube is incubated for 1 minute at room temperature before centrifuging it again at maximum speed for 10 minutes at 4 °C. After the centrifugation, a multi-layer suspension will form. The upper layer should be transferred into a new eppendorf in 20 µl increments (One should be careful not to touch the middle layer). The volume transferred should be recorded (V). To the eppendorf with the transferred Trizol, 0.7 V of isopropanol is added. Next, the eppendorf containing the transferred Trizol and isopropanol is incubated at room temperature for 10 minutes. Following the incubation, the eppendorf is centrifuged at maximum speed for 30 minutes at 4 °C. Next, an RNA pellet will be formed. The isopropanol (Sigma-Aldrich) above the pellet should be removed. To the RNA pellet 70%

ethanol is added (the volume of ethanol is the same volume of Trizol added in the beginning; approximately 300 μ l). The eppendorf containing the RNA and the ethanol is spun at maximum speed for 10 minutes at 4 °C. The ethanol is then removed. The RNA pellet is washed for a second time with 70% ethanol (Sigma Aldrich) (same volume as the previous wash) and spun at maximum speed for 10 minutes at 4 °C. The ethanol is also removed following the centrifugation and the pellet is air-dried under the fume hood for 5 minutes. The pellet is resuspended in 30 μ l Nuclease free water (Autoclaved milli-Q water) and flicked well. The RNA concentration and purity are quantified using a spectrophotometer (Denovix, Wilmington, DE).

2. *cDNA Synthesis*

cDNA synthesis was performed using the iScript (Bio-rad, Hercules, CA) cDNA synthesis kit. RNA product should be of a concentration of about 1000 ng/ ml, optimally. The reaction mix tubes are comprised of 4 μ l Reaction Mix, 1 μ l Reverse transcriptase, 1 μ l RNA and 14 μ l of Nuclease free water. Samples are put in a thermal cycler (Thermo electron corporation, Waltham,MA) with a protocol that includes: priming at 25 °C for 5 minutes, followed by reverse transcription at 46 °C for 20 minutes, then an inactivation of reverse transcription continue for 1 minute at 95 °C followed by a 4 °C hold .The cDNA end product can be stored at -20°C for later use.

3. Real-Time Polymerase Chain Reaction (Real Time PCR)

Real time PCR was performed to assess the level of antimicrobial peptides expression.

Drosomycin, *Diptericin* and *Tot A* are effectors expressed following activation of Toll, IMD and JAK-STAT pathways, respectively. Expression levels of the various AMP was normalized against the housekeeping gene *Ribosomal protein L11* (RpL11). The Forward and Reverse primers (Macrogen, Seoul, South Korea) sequences are shown in the Table 2.

Table 2. Sequences and annealing temperatures for PCR primers. The forward and the reverse primer sequences and annealing temperature are indicated. *Drosomycin* primer sequence was obtained from Sherri et al., 2018 (126, 127). *Diptericin*, *Tot A* and *RpL11* gene sequences were generated using NCBI primer blast.

Gene	Direction	Sequence	Annealing temperature
<i>Drosomycin</i>	Forward	5'- TACTTGTTTCGCCCTCTTCG -3'	57°C
<i>Drosomycin</i>	Reverse	5'- GTATCTTCCGGACAGGCAGT- 3	57°C
<i>Diptericin</i>	Forward	5'- CCGCAGTACCCACTCAATCT -3'	57°C
<i>Diptericin</i>	Reverse	5'- ACTGCAAAGCCAAAACCATC-3'	57°C
<i>Tot A</i>	Forward	5'- CCCAGTTTGACCCCTGAG-3'	57°C
<i>Tot A</i>	Reverse	5'- GCCCTTCACACCTGGAGA-3'	57°C
<i>RpL11</i>	Forward	5'-CGATCCCTCCATCGGTATCT -3'	57°C
<i>RpL 11</i>	Reverse	5'- GCCCTTCACACCTGGAGA -3'	57°C

4. *Relative Gene Expression Analysis*

Each PCR reaction tube contained 5 μ l SYBR green (Bio-Rad), 0.5 μ l of the Forward primer (diluted to a concentration of 10 picomole), 0.5 μ l of the Reverse primer (Diluted to a concentration of 10 picomole), and 4 μ l of cDNA (diluted in a concentration of 1:7).

Each sample was run in triplicates. Bio-RAD CFX96 Real time system was used for real time analysis. Relative gene expression was analyzed using the Livak and Schmittgen system (128). The assessment repeated for three biological replicates each biological group was RNA extracted from 25 adults.

5. *Statistical Analysis*

One-way Anova analysis followed by Tukey's multiple comparison test was used to analyze statistical significance for hemocyte count and GFP positive cell count. Unpaired t-test was used when comparing AMP relative expression. P-values lower than 0.05 were considered statistically significant. Statistics analysis was performed on a GraphPad Prism 6.0 program.

CHAPTER IV

RESULTS

A. Validation of *BCR-ABL*^{P210} and *BCR-ABL*^{T315I} Expression in Third-Instar Larval Hemocytes.

We validated the expression of *BCR-ABL*^{P210} and *BCR-ABL*^{T315I} in hemocytes using the *Hml Δ-Gal4; UAS-GFP* driver. Immunofluorescence imaging for Myc-BCR-ABL tag was assessed on larval bleed to detect its expression. As expected, in *BCR-ABL*^{P210} and *BCR-ABL*^{T315I} expressing flies, we detected Myc tag expression in GFP expressing hemocytes indicating the expression of the transgene in hemocytes. (Figure 6).

B. *BCR-ABL*^{P210} and *BCR-ABL*^{T315I} Expressing Flies Show Increase in Circulating Hemocyte Number.

In order to better understand the impact of expressing of *BCR-ABL*^{P210} and of *BCR-ABL*^{T315I} in hemocytes we carried on further phenotypic analyses. Expressing *BCR-ABL*^{P210} and of *BCR-ABL*^{T315I} in hemocytes using *Hml Δ-Gal4; UAS-GFP* resulted in increased circulating hemocyte number. The number of circulating hemocytes was determined using a hemocytometer where the average number of circulating hemocytes in control flies is 2.7×10^5 cells/ml, compared to 9.9×10^5 cells/ml in *BCR-ABL*^{P210} and 1.34×10^6 cells/ml in *BCR-ABL*^{T315I} expressing flies. The significance was assessed through one-way Anova test. The increase in hemocyte counts of *BCR-ABL*^{P210} and *BCR-ABL*^{T315I} compared to controls is highly significant with a p value ≤ 0.001 compared to control. Furthermore; *BCR-*

ABL^{T315I} exhibited a significantly higher hemocyte number compared to *BCR-ABL*^{P210}. The average number of hemocytes was obtained from three different biological replicates n=3 with ten third instar larvae for each replicate. Total number of larvae used in each condition (n=30) (Figure 7).

C. *BCR-ABL*^{P210} and *BCR-ABL*^{T315I} Expressing Flies Show an Increase in GFP Positive Hemocytes by Flow Cytometry.

To further validate the increase in circulating hemocytes observed by manual count using the hemocytometer we additionally performed flow cytometry analysis for GFP positive population of hemocytes. Similar to the increase observed above, we have noticed increase in hemocyte numbers in *BCR-ABL*^{P210} and *BCR-ABL*^{T315I} expressing flies compared to the control. The average number of GFP positive cells was obtained from 18 runs per genotype with 5 pooled larvae per run. The average GFP positive hemocyte population expressing green fluorescence greater than 10¹ was 51.1% in control flies, 59.4% in *BCR-ABL*^{P210} expressing flies and 60.04% in *BCR-ABL*^{T315I} expressing flies. Both *BCR-ABL*^{P210} and *BCR-ABL*^{T315I} were highly significant compared to the control with a p value ≤ 0.01 for *BCR-ABL*^{P210} and a p value ≤ 0.001 for *BCR-ABL*^{T315I} (Figure 8).

D. Disruption of Sessile Patterning in *BCR-ABL*^{P210} and *BCR-ABL*^{T315I} Expressing Larvae.

The defects observed in hemocyte number when expressing either *BCR-ABL*^{P210} or *BCR-ABL*^{T315I} raised the emphasis whether this increase is also reflected phenotypically and affects the regular banded pattern of the sessile hemocytes, depicted by an arrow in Figure

9 A. We analyzed 3rd instar larvae sessile hemocytes present under the larval epithelium of both *BCR-ABL*^{P210} and *BCR-ABL*^{T315I} expressing larval hemocytes. We indeed observed disrupted pattern in *BCR-ABL*^{P210} and *BCR-ABL*^{T315I} compared to control flies (Compare A to B and C). Worth noting that this disruption was different in *BCR-ABL*^{T315I} flies compared to *BCR-ABL*^{P210} indicated by the disappearance of distinct hemocytes and an overall diffused green signal (Compare arrow in C and arrow in B) (Figure 9).

E. Appearance of Melanotic Tumors in *BCR-ABL*^{T315I} but not in *BCR-ABL*^{P210} Expressing Larvae.

One of the hallmark observations upon overexpression of oncogenes is the appearance of melanotic tumors. Therefore; we further analyzed larvae expressing *BCR-ABL*^{P210} and *BCR-ABL*^{T315I} in hemocytes for the presence of melanotic tumors which usually appear like black nodules under the larval cuticle. Notably, melanotic tumors (depicted by arrowhead in Figure 10 C) appeared in 30% of 100 monitored *BCR-ABL*^{T315I} but not in any *BCR-ABL*^{P210} and control flies (Figure 10).

F. Assessing Humoral Immune Pathway Status in *BCR-ABL*^{P210} and *BCR-ABL*^{T315I} Expressing Flies.

Given the severe defects observed in the cellular arm of the innate immunity in *BCR-ABL*^{P210} and *BCR-ABL*^{T315I} expressing larvae, we further opted to examine the status of the three major humoral immune pathways, the Toll, IMD and JAK/STAT pathways. We aimed to detect the mRNA expression level of *Drosomycin*, *Diptericin* and *Tot A* the AMP indicative of humoral immune pathways involvement.

For *drosomycin*, relative expression was normalized to *RPL11* gene. Control flies had a relative expression of 1, *BCR-ABL*^{P210} expressing flies had a 1.2 relative expression, while *BCR-ABL*^{T3151} expressing flies showed 0.4 relative expression. There was a significant difference between control flies and *BCR-ABL*^{T3151} *drosomycin* relative expression with a P value of 0.0068 (Figure 11)

In a similar way, *dipteracin*, relative expression was normalized to *RPL11* gene. Control flies had 1 relative expression, *BCR-ABL*^{P210} expressing flies had a 2.4 relative expression, while *BCR-ABL*^{T3151} expressing flies showed a 0.99 relative expression. There was a significant difference between control flies and *BCR-ABL*^{P210} flies in *dipteracin* relative expression with a P value of 0.04 (Figure 12).

For *Tot A*, relative expression was normalized to *RPL11* gene. Control flies had 1 relative expression, *BCR-ABL*^{P210} expressing flies had a 5.1 relative expression, while *BCR-ABL*^{T3151} expressing flies showed a 66.7 relative expression. There was a significant difference between control flies and *BCR-ABL*^{T3151} expressing flies *Tot A* relative expression with a P value of 0.0022 (Figure 13).

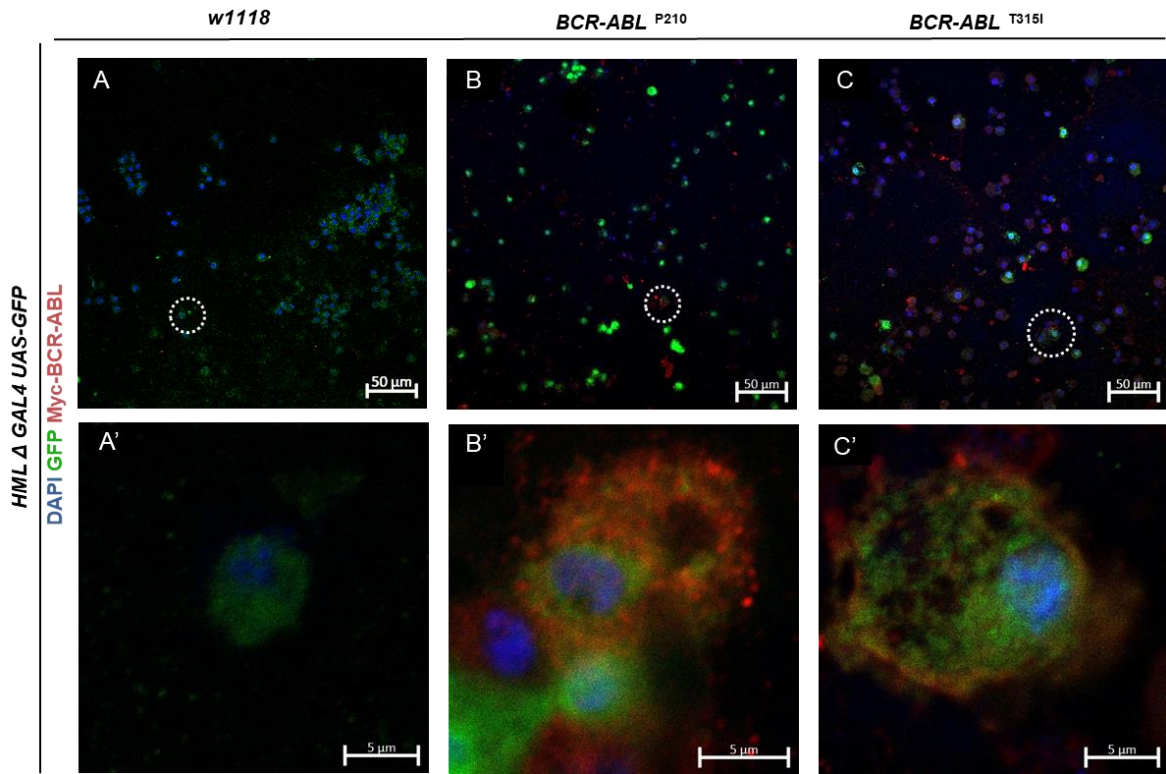


Figure 6. Immunofluorescence staining of larval bleed. (A-C) show 40X magnification of hemocytes from control (A), *BCR-ABL*^{P210} (B), and of *BCR-ABL*^{T315I} bleed (C). (A'-C') 63X magnification of single hemocytes from control (A') *BCR-ABL*^{P210} (B') and of *BCR-ABL*^{T315I} bleed (C'). Dashed circle in (A-C) indicates zoomed in cell in (A'-C') respectively with co-localization of three signals.

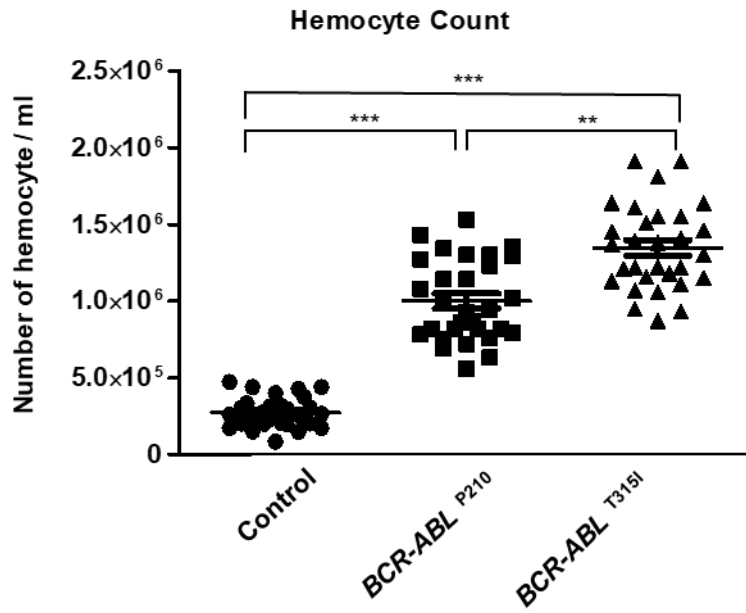


Figure 7. Hemocyte count in *BCR-ABL*^{P210} and *BCR-ABL*^{T315I} expressing larval bleed. The graph depicts the number of hemocytes in circulation obtained from 30 larvae per genotype. P value ≤ 0.001 is indicated by ***. P value ≤ 0.01 is indicated by **.

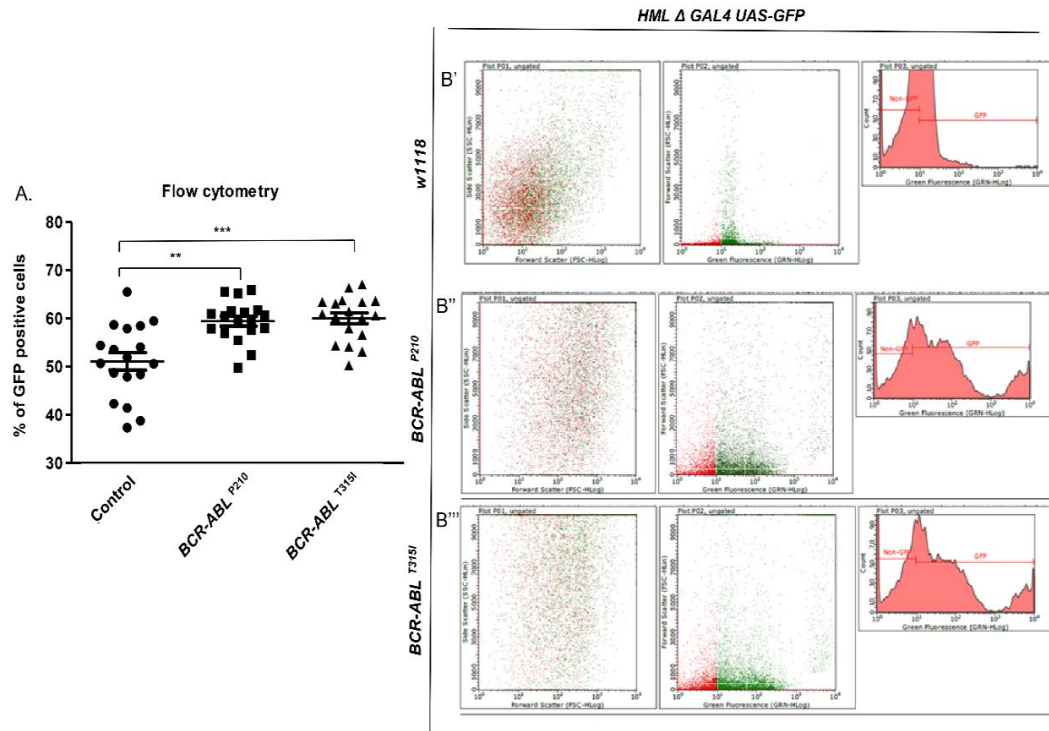


Figure 8. GFP positive hemocyte population in larval bleed expressing $BCR-ABL^{P210}$ and $BCR-ABL^{T315I}$. Graph depicts the number of GFP positive hemocytes in circulation obtained from 90 larvae per genotype (A). P value ≤ 0.001 is indicated by ***. P value ≤ 0.01 is indicated by **. First Plot 01 represents the forward scatter (X-axis) against the side scatter (Y-axis). Second Plot 02 represents the forward scatter (Y-axis) against the GFP fluorescence (Y-axis) of the events. Third Plot 03 represents green fluorescence against count. A representative image of the run for control flies (B') $BCR-ABL^{P210}$ flies (B'') and $BCR-ABL^{T315I}$ flies (B''').

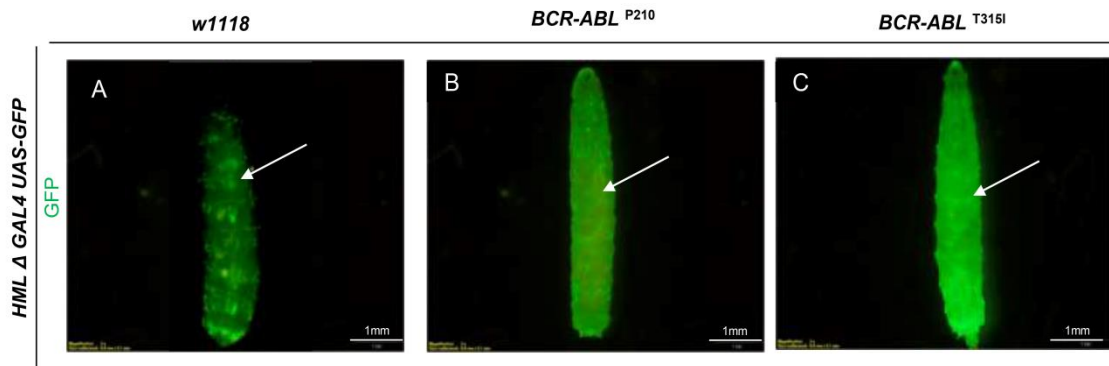


Figure 9. Disruption in sessile patterning in *BCR-ABL*^{P210} and *BCR-ABL*^{T315I} flies. Green fluorescence indicates endogenous GFP expressed in lymph gland and circulating hemocytes by *Hml Δ-Gal4; UAS-GFP* driver. A GFP image of control third instar larvae (A) *BCR-ABL*^{P210} third instar larvae (B) *BCR-ABL*^{T315I} third instar larvae (C). Arrow in (A) indicates normal sessile patterning. Arrow in (B) indicates disrupted sessile patterning but with few visible hemocytes. Arrow in (C) indicates total disruption of sessile patterning with no discernible hemocytes.

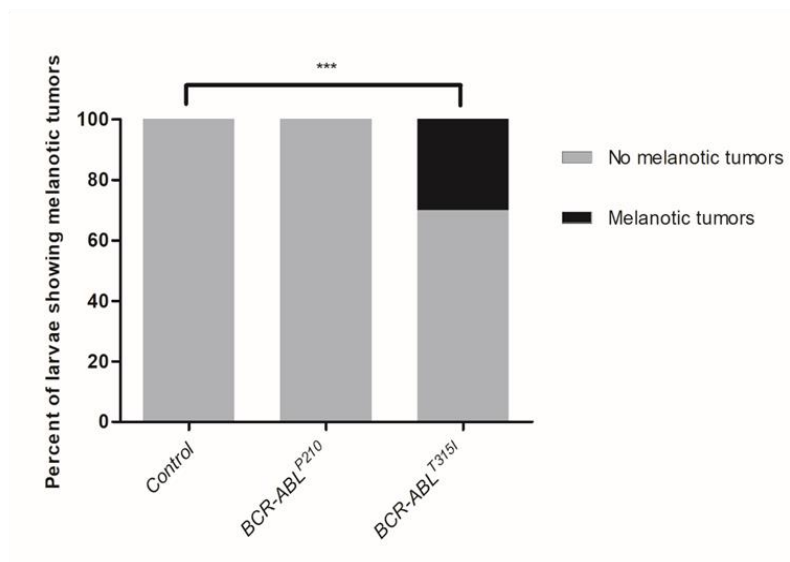
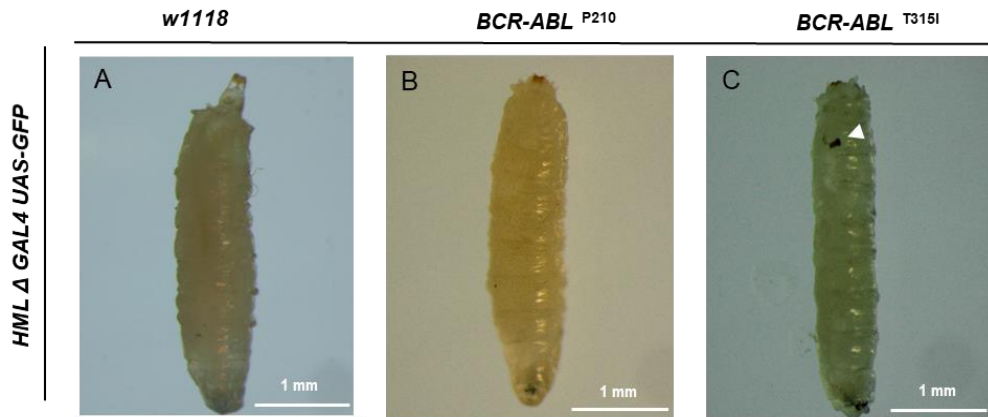


Figure 10. Melanotic tumors in *BCR-ABL*^{T315I} expressing 3rd instar larvae. The image shows control flies (A) *BCR-ABL*^{P210} (B) and *BCR-ABL*^{T315I} flies (C). Arrow head in (C) indicate melanotic tumors. The bar graph indicates the percentage of larvae exhibiting melanotic tumors n=100.

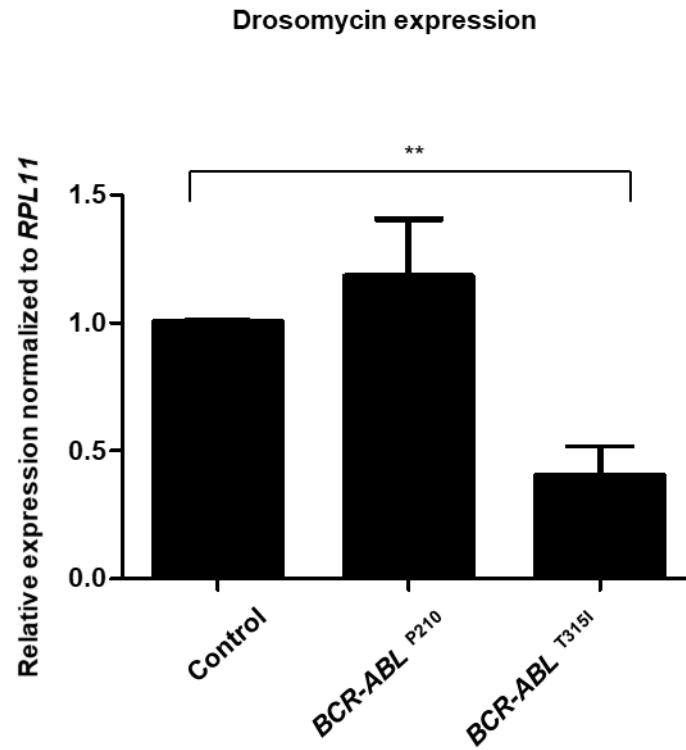


Figure 11. *Drosomycin* relative expression normalized to *RPL11*. P value ≤ 0.01 is indicated by **.

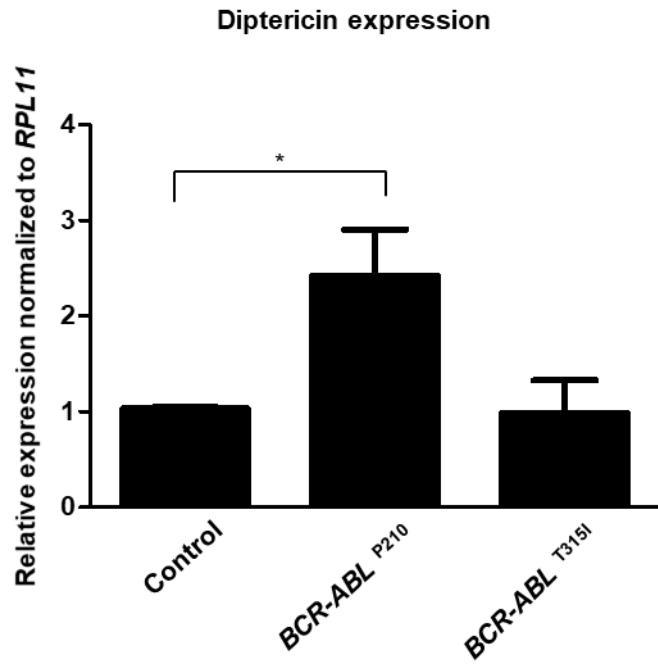


Figure 12. *Diptericin* relative expression normalized to *RPL11*. P value ≤ 0.05 is indicated by *.

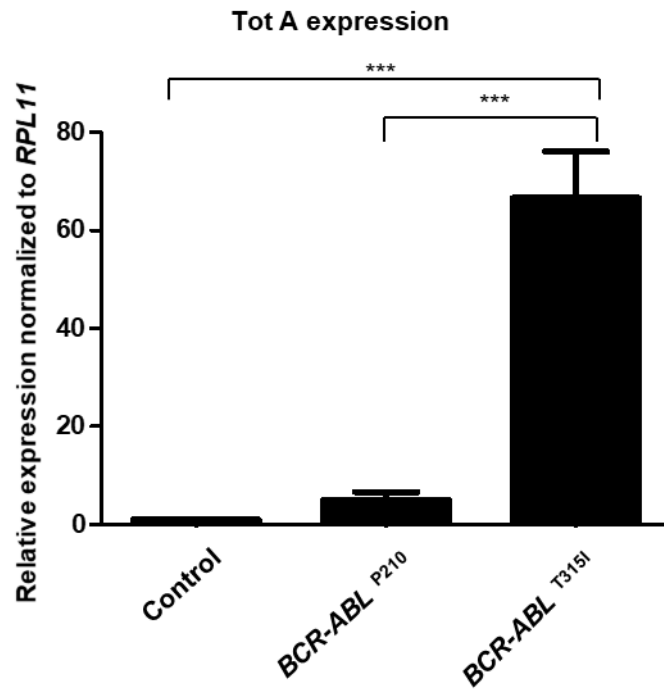


Figure 13. *Tot A* relative expression normalized to *RPL11*. P value ≤ 0.001 is indicated by ***.

CHAPTER V

DISCUSSION

Chronic myeloid leukemia (CML) is caused by a balanced chromosomal translocation resulting in the formation of *BCR-ABL* fusion gene that encodes a constitutively active BCR-ABL tyrosine kinase in a hematopoietic stem cell (HSC). This acquisition activates multiple signal transduction pathways leading to a transformation of the HSC into a leukemic stem cell (LSC) (2, 129). Several treatment modalities have been proposed to combat the tyrosine kinase activity of BCR-ABL, namely tyrosine kinase inhibitors (TKI). However, some mutations of the oncogene, especially the substitution of threonine with isoleucine on the 315th residue (T315I mutation), in addition to LSC, have proven resistant to most TKIs. In this research project we have used a previously established *Drosophila melanogaster* CML model in our lab to specifically assess the impact of expressing human *BCR-ABL* both wildtype *BCR-ABL*^{P210} and mutated *BCR-ABL*^{T315I} in the hematopoietic system using *Hml Δ-Gal4; UAS-GFP* which drives expression of transgenes in GFP labelled hemocytes.

We therefore first examined the number of circulating hemocytes in transgene expressing hemocytes through manual count using a hemocytometer. The expression of *BCR-ABL*^{P210} and mutated *BCR-ABL*^{T315I} resulted in a highly significant increase in the number of cells in the *Drosophila* bleed compared to the control. Interestingly, *BCR-ABL*^{T315I} exhibited a higher number of hemocytes slightly significant compared to the

wildtype *BCR-ABL*^{P210}. This was concurrent with appearance of melanotic tumors only in *BCR-ABL*^{T3151} expressing flies but not in *BCR-ABL*^{P210}. Both mutated *BCR-ABL*^{T3151} and *BCR-ABL*^{P210} showed a significant increase in the number of GFP positive cells compared to the control and a disruption in the sessile patterning of sub-epithelial hemocytes. However, unlike the manual count using the hemocytometer, there was no significant difference between mutated *BCR-ABL*^{T3151} and *BCR-ABL*^{P210} when examining the number of GFP positive cells. Moreover, the immunofluorescence experiment on *BCR-ABL*^{T3151} bleed showed cells that are DAPI positive only with no GFP or Myc co-localization (Arrow head in Figure 6 C). What these observations collectively could suggest is *BCR-ABL*^{T3151} induced the proliferation of prohemocyte population, a population that would not yet express the *Hemolectin* marker and thus would be a non-GFP population and forced their release in the circulation through a premature rupture of the lymph gland (130).

Moreover; the determination of the reason behind the increase in GFP cells in both *BCR-ABL*^{T3151} and *BCR-ABL*^{P210} compared to the control in the flow cytometry study would be difficult. However; there could be two hypotheses that might explain it. Either a premature hyperproliferation or rupture of the lymph gland or the mobilization of the sessile hemocytes could have both led to an increase in the GFP positive cells.

In addition, due to the observations we saw in the cellular arm of the innate immunity we wanted to evaluate the crosstalk between innate immune pathways and *BCR-ABL* mediated leukemogenesis in *Drosophila* females. We assessed the humoral innate immune response of *BCR-ABL*^{P210} and *BCR-ABL*^{T3151} expressing flies through measuring the transcript levels of the different AMP. Both *BCR-ABL*^{P210} and *BCR-ABL*^{T3151} showed

varying levels and sometimes opposing trends in AMP production when the different immune pathways were assessed. First, the assessment of *drosomycin* AMP transcript level showed a 77.8% decrease in *BCR-ABL*^{T315I} expressing flies compared to control flies. *BCR-ABL*^{P210} showed a slight non-significant increase. The decrease in *drosomycin* transcript level suggests the inhibition of the Toll pathway, which is homologous to the Toll-like receptor (TLR) pathway in mammals, in *BCR-ABL*^{T315I} but not *BCR-ABL*^{P210}. However, the assessment of *dipteracin* transcript level showed a 42.4% increase in the transcript level in *BCR-ABL*^{P210} expressing flies compared to control flies but no significant change was observed in *BCR-ABL*^{T315I}. This increase suggests that the IMD pathway response, which is homologous to the Tumor Necrosis Factor- α Receptor Signaling (TNFR) in mammals, is augmented in *BCR-ABL*^{P210} but not *BCR-ABL*^{T315I}. Finally, the transcript level of the *Tot A* AMP was assessed in *BCR-ABL*^{P210} and *BCR-ABL*^{T315I} expressing flies. In this condition both *BCR-ABL*^{P210} and *BCR-ABL*^{T315I} showed an increase in *Tot A* transcript level. This suggests that the JAK-STAT pathway is activated in both *BCR-ABL*^{P210} and *BCR-ABL*^{T315I} with a greater augmented response in *BCR-ABL*^{T315I}. However, in a paper that co-cultured human mesenchymal stem-cells bone marrow (HMSC-BM) with Ph⁺ K-562 CML cells, MyD88 levels were upregulated in K-562 co-cultured HMSC-BM compared to HMSC-BM controls. While, NF- κ B expression was not different between K-562 co-cultured HMSC-BM compared to the control (131).

The differential findings between *BCR-ABL*^{P210} and *BCR-ABL*^{T315I} could be attributed to their diverse mediation of signaling pathways. Until very recently the presence of BCR-ABL alone was thought to be enough to provide HSC with an oncogenic and

transformation potential (132). However, more research is pointing at the importance of *BCR-ABL* copy number, secondary mutations that could arise inside or outside the ABL kinase domain as well as genomic stability in inducing leukemogenesis (133). Thus, what can be predicted is that *BCR-ABL*^{P210} on its own may not have produced the full leukemic potential of *BCR-ABL*^{T315I}. This rationale could be the reason why there was a significant increase in the number of circulating hemocytes and varying innate immune response between *BCR-ABL*^{P210} and *BCR-ABL*^{T315I}. In addition, the presence of the T315I mutation introduced through T315I⁺ vectors into animal models conferred additional oncogenicity and led to an increased growth in the bone marrow compared to *BCR-ABL*^{P210} (134). Interestingly, this increased oncogenic potential was not correlated with an increase in the tyrosine kinase activity of *BCR-ABL*^{T315I} (134). One of the proposed mechanisms for T315I oncogenic advantage is the activation of Ras/MAPK pathway acting via the human estrogen receptor alpha 6 (ER α 6) signaling (135, 136). It was found that (ER α 6) promoted cell growth and inhibited apoptosis in *BCR-ABL*^{T315I} positive cell lines by phosphorylating Tyr 177 residue on BCR promoted the binding to GRB2 to the BCR-ABL, and formation of the BCR-ABL/SOS/GRB2 complex which in turn activated the Ras/ MAPK pathway (135). The Ras/ MAPK was also shown to suppress the *Drosophila* IMD/NF- κ B signaling (137). However, activation of NF- κ B signaling has been shown to induce resistance to apoptosis in hematological malignancies (138). Therefore, it is possible that *BCR-ABL*^{T315I} exhibited a higher activity rate of Ras/ MAPK compared to *BCR-ABL*^{P210} and this higher Ras/MAPK activity levels suppressed the IMD/NF- κ B activation. Thus, *diptericin* transcript levels were only upregulated in *BCR-ABL*^{P210}. Moreover, Toll pathway signaling is known to be initiator of the NF- κ B signaling cascade. For example, lipopolysaccharides

(LPS) bind to the TLR-4 which activated the NF- κ B pathway (139). This could explain the reason behind similar trends observed in *drosomycin* and *diptericin* expression in *BCR-ABL*^{P210} and *BCR-ABL*^{T315I} expressing flies. On the other hand, JAK/ STAT pathway has been studied extensively in CML. STAT5 was shown to maintain the survival and growth of CML cells. In addition, JAK2 has been correlated with increased LSC persistence in TKI background (140). Additionally, Src inhibitors have been shown to lower p-STAT5 in *BCR-ABL*^{P210} but not in *BCR-ABL*^{T315I}. This could suggest an over activation in the JAK/STAT pathway that the Src inhibitors (PP1 and CGP76030) could not overcome in *BCR-ABL*^{T315I} (141). The role of JAK/STAT pathway in CML persistence could explain the increased *Tot A* transcript level in both *BCR-ABL*^{P210} and *BCR-ABL*^{T315I}. Moreover, the hyperactivation of JAK/STAT pathway in *BCR-ABL*^{T315I} could explain the higher *Tot A* transcript levels compared to *BCR-ABL*^{P210}. However, our examination of the humoral arm of *Drosophila* innate immunity through assessing the mRNA levels of effector genes provided an initial insight into the signaling complexity mediated by wild type and mutated *BCR-ABL*. Further assessment of the activity of candidate pathways acting upstream of the oncogene are needed to obtain a full understanding of the leukemogenic potential of *BCR-ABL*^{P210} and *BCR-ABL*^{T315I}.

A. Limitations and Future Perspectives

In this research project, we attained the first steps needed to establish a *D. melanogaster* hematopoietic model for CML. Several objectives were met in this project, however, it still falls short in some aspects that would require further research. *Drosophila melanogaster* does not harbor adaptive immunity necessary to combat BCR-ABL mediated oncogenesis.

Moreover, Natural killer cells which are important mediators in immunity in CML patients are absent in *Drosophila melanogaster*.

However, this research project set the primary pedestal for a genetic screening line to understand the pathways mediating the phenotypes we have observed upon the expression of both *BCR-ABL*^{P210} and *BCR-ABL*^{T315I}. The *BCR-ABL*^{T315I} in comparison to *BCR-ABL*^{P210} transcriptome analysis would allow to study if any secondary mutations or epigenetic changes have occurred in *BCR-ABL*^{T315I} and mediated their differential phenotype compared to *BCR-ABL*^{P210}. Based on previous research in our laboratory *D. melanogaster* was validated as drug screening model for TKIs. Thus, this hematopoietic model would serve as a secondary drug screening line to validate the therapeutic potential of candidate drugs.

B. Conclusion

In conclusion, our findings helped establish a hematological model for CML through expressing *BCR-ABL*^{P210} and *BCR-ABL*^{T315I} in the *Drosophila* hematopoietic system. The expression of *BCR-ABL*^{P210} and *BCR-ABL*^{T315I} led to an increase in the number of hemocytes found in the hemolymph of both genotypes compared to control flies, with a greater increase in the number of hemocytes and the appearance of melanotic tumors in the *BCR-ABL*^{T315I} expressing flies compared to the *BCR-ABL*^{P210}. However, this increase was not exactly recapitulated by a difference in the number of GFP positive cells between *BCR-ABL*^{P210} and *BCR-ABL*^{T315I}. This suggested that *BCR-ABL*^{T315I} promoted the expression of certain hemocyte population(s) which were not GFP positive. In addition, the differential

expression of AMP between *BCR-ABL*^{P210} and *BCR-ABL*^{T315I} suggested a difference in their signaling fingerprint. *BCR-ABL*^{P210} showed an activation of the IMD pathway while *BCR-ABL*^{T315I} showed a downregulation of the Toll pathway and activation of the JAK-STAT pathway. Our findings assert the need for further investigations regarding the differences between *BCR-ABL*^{P210} and *BCR-ABL*^{T315I} and the method *BCR-ABL*^{T315I} confers a fitness advantage toward leukemogenesis and drug resistance. Filling these gaps would help to find both curative route for CML and methods to overcome leukemic stem cells persistence.

BIBLIOGRAPHY

1. Jabbour E, Kantarjian H. Chronic myeloid leukemia: 2018 update on diagnosis, therapy and monitoring. *American Journal of Hematology*. 2018;93(3):442-59.
2. Nowell PC, Nowell PC, Hungerford DA, Hungerford DA. Chromosome 1960;25(1):85-109.
3. Rowley JD. A new consistent chromosomal abnormality in chronic myelogenous leukaemia identified by quinacrine fluorescence and Giemsa staining. *Nature*. 1973;243(5405):290.
4. Lugo T, Pendergast A, Muller A, Witte O. Tyrosine kinase activity and transformation potency of bcr-abl oncogene products. *Science*. 1990;247(4946):1079-82.
5. Melo J. The diversity of BCR-ABL fusion proteins and their relationship to leukemia phenotype [editorial; comment]. *Blood*. 1996;88(7):2375-84.
6. Pendergast AM, Muller AJ, Havlik MH, Maru Y, Witte ON. BCR sequences essential for transformation by the BCR-ABL oncogene bind to the ABL SH2 regulatory domain in a non-phosphotyrosine-dependent manner. *Cell*. 1991;66(1):161-71.
7. Perrotti D, Jamieson C, Goldman J, Skorski T. Chronic myeloid leukemia: mechanisms of blastic transformation. *The Journal of Clinical Investigation*. 2010;120(7):2254-64.
8. Cross NCP, Daley GQ, Green AR, Hughes TP, Jamieson C, Manley P, et al. BCR-ABL1-positive CML and BCR-ABL1-negative chronic myeloproliferative disorders: some common and contrasting features. *Leukemia*. 2008;22:1975.
9. Pendergast AM, Quilliam LA, Cripe LD, Bassing CH, Dai Z, Li N, et al. BCR-ABL-induced oncogenesis is mediated by direct interaction with the SH2 domain of the GRB-2 adaptor protein. *Cell*. 1993;75(1):175-85.
10. Melo JV, Deininger MWN. Biology of chronic myelogenous leukemia—signaling pathways of initiation and transformation. *Hematology/Oncology Clinics of North America*. 2004;18(3):545-68.
11. Zhang X, Subrahmanyam R, Wong R, Gross AW, Ren R. The NH2-Terminal Coiled-Coil Domain and Tyrosine 177 Play Important Roles in Induction of a Myeloproliferative Disease in Mice by Bcr-Abl. *Molecular and Cellular Biology*. 2001;21(3):840-53.
12. Cortez D, Reuther G, Pendergast AM. The Bcr-Abl tyrosine kinase activates mitogenic signaling pathways and stimulates G1-to-S phase transition in hematopoietic cells. *Oncogene*. 1997;15(19):2333.
13. Ren R. Mechanisms of BCR-ABL in the pathogenesis of chronic myelogenous leukaemia. *Nature Reviews Cancer*. 2005;5(3):172.
14. Skorski T, Kanakaraj P, Nieborowska-Skorska M, Ratajczak MZ, Wen SC, Zon G, et al. Phosphatidylinositol-3 kinase activity is regulated by BCR/ABL and is required for the growth of Philadelphia chromosome-positive cells. *Blood*. 1995;86(2):726.
15. Franke TF, Kaplan DR, Cantley LC. PI3K: downstream AKTion blocks apoptosis. *Cell*. 1997;88(4):435-7.

16. Carlesso N, Frank DA, Griffin JD. Tyrosyl phosphorylation and DNA binding activity of signal transducers and activators of transcription (STAT) proteins in hematopoietic cell lines transformed by Bcr/Abl. *The Journal of Experimental Medicine*. 1996;183(3):811.
17. O'Brien SG, Guilhot F, Larson RA, Gathmann I, Baccarani M, Cervantes F, et al. Imatinib Compared with Interferon and Low-Dose Cytarabine for Newly Diagnosed Chronic-Phase Chronic Myeloid Leukemia. *The New England Journal of Medicine*. 2003;348(11):994-1004.
18. Druker BJ, Guilhot F, O'Brien SG, Gathmann I, Kantarjian H, Gattermann N, et al. Five-Year Follow-up of Patients Receiving Imatinib for Chronic Myeloid Leukemia. *The New England Journal of Medicine*. 2006;355(23):2408-17.
19. Iacobucci I, Saglio G, Rosti G, Testoni N, Pane F, Amabile M, et al. Achieving a major molecular response at the time of a complete cytogenetic response (CCgR) predicts a better duration of CCgR in imatinib-treated chronic myeloid leukemia patients. *Clinical Cancer Research*. 2006;12(10):3037-42.
20. Hochhaus A, Baccarani M, Deininger M, Apperley JF, Lipton JH, Goldberg SL, et al. Dasatinib induces durable cytogenetic responses in patients with chronic myelogenous leukemia in chronic phase with resistance or intolerance to imatinib. *Leukemia*. 2008;22(6):1200-6.
21. O'Hare T, Deininger MWN, Eide CA, Clackson T, Druker BJ. Targeting the BCR-ABL signaling pathway in therapy-resistant Philadelphia chromosome-positive leukemia. *Clinical Cancer Research*. 2011;17(2):212-21.
22. Barouch-Bentov R, Sauer K. Mechanisms of drug resistance in kinases. *Expert Opinion on Investigational Drugs*. 2011;20(2):153-208.
23. Chan Wayne W, Wise Scott C, Kaufman Michael D, Ahn Yu M, Ensinger Carol L, Haack T, et al. Conformational Control Inhibition of the BCR-ABL1 Tyrosine Kinase, Including the Gatekeeper T315I Mutant, by the Switch-Control Inhibitor DCC-2036. *Cancer Cell*. 2011;19(4):556-68.
24. Tanaka R, Squires MS, Kimura S, Yokota A, Nagao R, Yamauchi T, et al. Activity of the multitargeted kinase inhibitor, AT9283, in imatinib-resistant BCR-ABL-positive leukemic cells. *Blood*. 2010;116(12):2089-95.
25. Gd M, Bj B, Cs L. Resistant mutations in CML and Ph+ALL - role of ponatinib. *Biologics : Targets & Therapy*. 2014;2014(default):243-54.
26. Sontakke P, Jaques J, Vellenga E, Schuringa JJ. Modeling of Chronic Myeloid Leukemia: An Overview of In Vivo Murine and Human Xenograft Models. *Stem cells international*. 2016;2016:1625015-.
27. Jennings BH. *Drosophila – a versatile model in biology & medicine*. *Materials Today*. 2011;14(5):190-5.
28. Pandey UB, Nichols CD. Human disease models in *Drosophila melanogaster* and the role of the fly in therapeutic drug discovery. *Pharmacol Rev*. 2011;63(2):411-36.
29. Rizki T. circulatory system and associated cells and tissues. *Genetics and biology of Drosophila*. 1978.

30. Franc NC. Phagocytosis of apoptotic cells in mammals, *Caenorhabditis elegans* and *Drosophila melanogaster*: molecular mechanisms and physiological consequences. *Front Biosci.* 2002;7:1298-313.
31. Agaisse H, Petersen U-M, Boutros M, Mathey-Prevoit B, Perrimon N. Signaling Role of Hemocytes in *Drosophila* JAK/STAT-Dependent Response to Septic Injury. *Developmental Cell.* 2003;5(3):441-50.
32. Freeman MR, Delrow J, Kim J, Johnson E, Doe CQ. Unwrapping glial biology: Gcm target genes regulating glial development, diversification, and function. *Neuron.* 2003;38(4):567-80.
33. Fadok VA, Bratton DL, Rose DM, Pearson A, Ezekowitz RAB, Henson PM. A receptor for phosphatidylserine-specific clearance of apoptotic cells. *Nature.* 2000;405(6782):85.
34. Franc NC, Dimarcq J-L, Lagueux M, Hoffmann J, Ezekowitz RAB. Croquemort, a novel *Drosophila* hemocyte/macrophage receptor that recognizes apoptotic cells. *Immunity.* 1996;4(5):431-43.
35. Watson FL, Püttmann-Holgado R, Thomas F, Lamar DL, Hughes M, Kondo M, et al. Extensive diversity of Ig-superfamily proteins in the immune system of insects. *Science.* 2005;309(5742):1874-8.
36. Kurucz É, Márkus R, Zsámboki J, Folkl-Medzihradzky K, Darula Z, Vilmos P, et al. Nimrod, a putative phagocytosis receptor with EGF repeats in *Drosophila* plasmatocytes. *Current Biology.* 2007;17(7):649-54.
37. Kocks C, Cho JH, Nehme N, Ulvila J, Pearson AM, Meister M, et al. Eater, a Transmembrane Protein Mediating Phagocytosis of Bacterial Pathogens in *Drosophila*. *Cell.* 2005;123(2):335-46.
38. Rizki T, Rizki RM, Bellotti R. Genetics of a *Drosophila* phenoloxidase. *Molecular and General Genetics MGG.* 1985;201(1):7-13.
39. Chosa N, Fukumitsu T, Fujimoto K, Ohnishi E. Activation of prophenoloxidase A1 by an activating enzyme in *Drosophila melanogaster*. *Insect biochemistry and molecular biology.* 1997;27(1):61-8.
40. De Gregorio E, Han S-J, Lee W-J, Baek M-J, Osaki T, Kawabata S-I, et al. An immune-responsive Serpin regulates the melanization cascade in *Drosophila*. *Developmental cell.* 2002;3(4):581-92.
41. Castillejo-López C, Häcker U. The serine protease Sp7 is expressed in blood cells and regulates the melanization reaction in *Drosophila*. *Biochemical and biophysical research communications.* 2005;338(2):1075-82.
42. Bidla G, Lindgren M, Theopold U, Dushay MS. Hemolymph coagulation and phenoloxidase in *Drosophila* larvae. *Developmental & Comparative Immunology.* 2005;29(8):669-79.
43. Rizki TM, Rizki RM. Lamellocyte differentiation in *Drosophila* larvae parasitized by *Leptopilina*. *Developmental & Comparative Immunology.* 1992;16(2):103-10.
44. Lanot R, Zachary D, Holder F, Meister M. Postembryonic Hematopoiesis in *Drosophila*. *Developmental Biology.* 2001;230(2):243-57.
45. Cumano A, Godin I. Ontogeny of the hematopoietic system. *Annu Rev Immunol.* 2007;25:745-85.

46. Lebestky T, Chang T, Hartenstein V, Banerjee U. Specification of *Drosophila* hematopoietic lineage by conserved transcription factors. *Science*. 2000;288(5463):146-9.
47. Dzierzak E. The emergence of definitive hematopoietic stem cells in the mammal. *Current opinion in hematology*. 2005;12(3):197-202.
48. Tepass U, Fessler LI, Aziz A, Hartenstein V. Embryonic origin of hemocytes and their relationship to cell death in *Drosophila*. *Development*. 1994;120(7):1829-37.
49. Rugendorff A, Younossi-Hartenstein A, Hartenstein V. Embryonic origin and differentiation of the *Drosophila* heart. *Roux's archives of developmental biology*. 1994;203(5):266-80.
50. Jung S-H, Evans CJ, Uemura C, Banerjee U. The *Drosophila* lymph gland as a developmental model of hematopoiesis. *Development*. 2005;132(11):2521.
51. Holz A, Bossinger B, Strasser T, Janning W, Klapper R. The two origins of hemocytes in *Drosophila*. *Development*. 2003;130(20):4955-62.
52. Rehorn K-P, Thelen H, Michelson AM, Reuter R. A molecular aspect of hematopoiesis and endoderm development common to vertebrates and *Drosophila*. *Development*. 1996;122(12):4023-31.
53. Patient RK, McGhee JD. The GATA family (vertebrates and invertebrates). *Current opinion in genetics & development*. 2002;12(4):416-22.
54. Chen J, Call GB, Beyer E, Bui C, Cespedes A, Chan A, et al. Discovery-based science education: functional genomic dissection in *Drosophila* by undergraduate researchers. *PLoS biology*. 2005;3(2):e59.
55. Cho NK, Keyes L, Johnson E, Heller J, Ryner L, Karim F, et al. Developmental control of blood cell migration by the *Drosophila* VEGF pathway. *Cell*. 2002;108(6):865-76.
56. Hosoya T, Takizawa K, Nitta K, Hotta Y. glial cells missing: a binary switch between neuronal and glial determination in *Drosophila*. *Cell*. 1995;82(6):1025-36.
57. Bataillé L, Augé B, Ferjoux G, Haenlin M, Waltzer L. Resolving embryonic blood cell fate choice in *Drosophila*: interplay of GCM and RUNX factors. *Development*. 2005;132(20):4635-44.
58. Wood W, Faria C, Jacinto A. Distinct mechanisms regulate hemocyte chemotaxis during development and wound healing in *Drosophila melanogaster*. *The Journal of cell biology*. 2006;173(3):405-16.
59. Reimels TA, Pflieger CM. Methods to Examine the Lymph Gland and Hemocytes in *Drosophila* Larvae. *Journal of visualized experiments : JoVE*. 2016(117):54544.
60. Mandal L, Banerjee U, Hartenstein V. Evidence for a fruit fly hemangioblast and similarities between lymph-gland hematopoiesis in fruit fly and mammal aorta-gonadal-mesonephros mesoderm. *Nature Genetics*. 2004;36:1019.
61. Benmimoun B, Polesello C, Haenlin M, Waltzer L. The EBF transcription factor Collier directly promotes *Drosophila* blood cell progenitor maintenance independently of the niche. *Proceedings of the National Academy of Sciences of the United States of America*. 2015;112(29):9052-7.

62. Bourbon H-M, Gonzy-Treboul G, Peronnet F, Alin M-F, Ardourel C, Benassayag C, et al. A P-insertion screen identifying novel X-linked essential genes in *Drosophila*. *Mechanisms of Development*. 2002;110(1):71-83.
63. Goto A, Kadowaki T, Kitagawa Y. *Drosophila* hemolectin gene is expressed in embryonic and larval hemocytes and its knock down causes bleeding defects. Two hml-GAL4 lines (w1118; P{w + mc = GAL4-Hml} 5-6 and w1118; P{w + mc = GAL4-Hml} 6-4) and one homozygote of d-hml-GAL4, UAS-gfpnlacZ, UAS-gfp[S65T]/d-hml-GAL4, UAS-gfpnlacZ, UAS-gfp[S65T] (w1118; P{w + mc = GAL4-Hml} 6-4 P{w + mc = UAS-GFP::lacZ.nls} 15.1) transgenic lines are available from the Bloomington Stock Center with the stock numbers of 6395, 6396, and 6397, respectively. *Developmental Biology*. 2003;264(2):582-91.
64. Nelson RE, Fessler LI, Takagi Y, Blumberg B, Keene DR, Olson PF, et al. Peroxidase: a novel enzyme-matrix protein of *Drosophila* development. *The EMBO journal*. 1994;13(15):3438-47.
65. Mandal L, Martinez-Agosto JA, Evans CJ, Hartenstein V, Banerjee U. A Hedgehog- and Antennapedia-dependent niche maintains *Drosophila* haematopoietic precursors. *Nature*. 2007;446:320.
66. Crozatier M, Ubeda J-M, Vincent A, Meister M. Cellular Immune Response to Parasitization in *Drosophila* Requires the EBF Orthologue Collier. *PLOS Biology*. 2004;2(8):e196.
67. Krzemiński J, Dubois L, Makki R, Meister M, Vincent A, Crozatier M. Control of blood cell homeostasis in *Drosophila* larvae by the posterior signalling centre. *Nature*. 2007;446:325.
68. Grigorian M, Mandal L, Hartenstein V. Hematopoiesis at the onset of metamorphosis: terminal differentiation and dissociation of the *Drosophila* lymph gland. *Development Genes and Evolution*. 2011;221(3):121-31.
69. Ghosh S, Singh A, Mandal S, Mandal L. Active Hematopoietic Hubs in *Drosophila* Adults Generate Hemocytes and Contribute to Immune Response. *Developmental Cell*. 2015;33(4):478-88.
70. SHRESTHA R, GATEFF E. Ultrastructure and Cytochemistry of the Cell Types in the Larval Hematopoietic Organs and Hemolymph of *Drosophila Melanogaster*: (*drosophila/hematopoiesis/blood cells/ultrastructure/cytochemistry*). *Development, Growth & Differentiation*. 1982;24(1):65-82.
71. Lanot R, Zachary D, Holder F, Meister M. Postembryonic Hematopoiesis in *Drosophila*, *De velop. Biol*; 2001.
72. Makhijani K, Alexander B, Tanaka T, Rulifson E, Brückner K. The peripheral nervous system supports blood cell homing and survival in the *Drosophila* larva. *Development*. 2011;138(24):5379-91.
73. Williams MJ, Wiklund M-L, Wikman S, Hultmark D. Rac1 signalling in the *Drosophila* larval cellular immune response. *Journal of cell science*. 2006;119(10):2015-24.
74. Bretscher AJ, Honti V, Binggeli O, Burri O, Poidevin M, Kurucz É, et al. The Nimrod transmembrane receptor Eater is required for hemocyte attachment to the sessile compartment in *Drosophila melanogaster*. *Biology open*. 2015;4(3):355-63.
75. Leitao AB, Sucena E. *Drosophila* sessile hemocyte clusters are true hematopoietic tissues that regulate larval blood cell differentiation. *Elife*. 2015;4:e06166.

76. Honti V, Kurucz É, Csordás G, Laurinyecz B, Márkus R, Andó I. In vivo detection of lamellocytes in *Drosophila melanogaster*. *Immunology letters*. 2009;126(1-2):83-4.
77. Avet-Rochex A, Boyer K, Polesello C, Gobert V, Osman D, Roch F, et al. An in vivo RNA interference screen identifies gene networks controlling *Drosophila melanogaster* blood cell homeostasis. *BMC developmental biology*. 2010;10(1):65.
78. Schmid MR, Anderl I, Vo HT, Valanne S, Yang H, Kronhamn J, et al. Genetic screen in *Drosophila* larvae links *ird1* function to toll signaling in the fat body and hemocyte motility. *PloS one*. 2016;11(7):e0159473.
79. Anderl I, Vesala L, Ihalainen TO, Vanha-aho L-M, Andó I, Rämetsä M, et al. Transdifferentiation and proliferation in two distinct hemocyte lineages in *Drosophila melanogaster* larvae after wasp infection. *PLoS pathogens*. 2016;12(7):e1005746.
80. Babcock DT, Brock AR, Fish GS, Wang Y, Perrin L, Krasnow MA, et al. Circulating blood cells function as a surveillance system for damaged tissue in *Drosophila* larvae. *Proceedings of the National Academy of Sciences*. 2008;105(29):10017-22.
81. Banerjee U, Girard JR, Goins LM, Spratford CM. *Drosophila* as a genetic model for hematopoiesis. *Genetics*. 2019;211(2):367-417.
82. Cordero JB, Macagno JP, Stefanatos RK, Strathdee KE, Cagan RL, Vidal M. Oncogenic Ras diverts a host TNF tumor suppressor activity into tumor promoter. *Developmental cell*. 2010;18(6):999-1011.
83. Pastor-Pareja JC, Wu M, Xu T. An innate immune response of blood cells to tumors and tissue damage in *Drosophila*. *Disease models & mechanisms*. 2008;1(2-3):144-54.
84. Kim MJ, Choe K-M. Basement membrane and cell integrity of self-tissues in maintaining *Drosophila* immunological tolerance. *PLoS genetics*. 2014;10(10):e1004683.
85. Osman D, Gobert V, Ponthan F, Heidenreich O, Haenlin M, Waltzer L. A *Drosophila* model identifies calpains as modulators of the human leukemogenic fusion protein AML1-ETO. *Proceedings of the National Academy of Sciences*. 2009;106(29):12043-8.
86. Sinenko SA, Hung T, Moroz T, Tran Q-M, Sidhu S, Cheney MD, et al. Genetic manipulation of AML1-ETO-induced expansion of hematopoietic precursors in a *Drosophila* model. *Blood*. 2010;116(22):4612-20.
87. Reitman ZJ, Sinenko SA, Spana EP, Yan H. Genetic dissection of leukemia-associated IDH1 and IDH2 mutants and D-2-hydroxyglutarate in *Drosophila*. *Blood*. 2015;125(2):336-45.
88. Qiu P, Pan PC, Govind S. A role for the *Drosophila* Toll/Cactus pathway in larval hematopoiesis. *Development*. 1998;125(10):1909-20.
89. Luo H, Hanratty W, Dearolf C. An amino acid substitution in the *Drosophila* hopTum-1 Jak kinase causes leukemia-like hematopoietic defects. *The EMBO journal*. 1995;14(7):1412-20.
90. Harrison DA, Binari R, Nahreini TS, Gilman M, Perrimon N. Activation of a *Drosophila* Janus kinase (JAK) causes hematopoietic neoplasia and developmental defects. *The EMBO Journal*. 1995;14(12):2857-65.

91. Gerttula S, Jin Y, Anderson KV. Zygotic expression and activity of the *Drosophila* Toll gene, a gene required maternally for embryonic dorsal-ventral pattern formation. *Genetics*. 1988;119(1):123-33.
92. Govind S. Control of development and immunity by rel transcription factors in *Drosophila*. *Oncogene*. 1999;18(49):6875.
93. Hoffmann JA. The immune response of *Drosophila*. *Nature*. 2003;426(6962):33.
94. Hultmark D. *Drosophila* immunity: paths and patterns. *Current opinion in immunology*. 2003;15(1):12-9.
95. Lemaitre B, Hoffmann J. The host defense of *Drosophila melanogaster*. *Annu Rev Immunol*. 2007;25:697-743.
96. Khush RS, Cornwell WD, Uram JN, Lemaitre B. A ubiquitin-proteasome pathway represses the *Drosophila* immune deficiency signaling cascade. *Current Biology*. 2002;12(20):1728-37.
97. Lagueux M, Perrodou E, Levashina EA, Capovilla M, Hoffmann JA. Constitutive expression of a complement-like protein in toll and JAK gain-of-function mutants of *Drosophila*. *Proceedings of the National Academy of Sciences*. 2000;97(21):11427-32.
98. Agaisse H, Petersen U-M, Boutros M, Mathey-Prevot B, Perrimon N. Signaling role of hemocytes in *Drosophila* JAK/STAT-dependent response to septic injury. *Developmental cell*. 2003;5(3):441-50.
99. Wang LD, Wagers AJ. Dynamic niches in the origination and differentiation of haematopoietic stem cells. *Nature reviews Molecular cell biology*. 2011;12(10):643.
100. Oh IH, Humphries RK. Concise review: multidimensional regulation of the hematopoietic stem cell state. *Stem Cells*. 2012;30(1):82-8.
101. Lacronique V, Boureux A, Della Valle V, Poirel H, Quang CT, Mauchauffé M, et al. A TEL-JAK2 fusion protein with constitutive kinase activity in human leukemia. *Science*. 1997;278(5341):1309-12.
102. Lee HJ, Daver N, Kantarjian HM, Verstovsek S, Ravandi F. The role of JAK pathway dysregulation in the pathogenesis and treatment of acute myeloid leukemia. *Clinical Cancer Research*. 2013;19(2):327-35.
103. Ekas LA, Cardozo TJ, Flaherty MS, McMillan EA, Gonsalves FC, Bach EA. Characterization of a dominant-active STAT that promotes tumorigenesis in *Drosophila*. *Developmental biology*. 2010;344(2):621-36.
104. Tanigaki K, Honjo T. Regulation of lymphocyte development by Notch signaling. *Nature immunology*. 2007;8(5):451.
105. Radtke F, Wilson A, MacDonald HR. Notch signaling in hematopoiesis and lymphopoiesis: lessons from *Drosophila*. *Bioessays*. 2005;27(11):1117-28.
106. Krzemiń J, Dubois L, Makki R, Meister M, Vincent A, Crozatier M. Control of blood cell homeostasis in *Drosophila* larvae by the posterior signalling centre. *Nature*. 2007;446(7133):325.
107. Mukherjee T, Kim WS, Mandal L, Banerjee U. Interaction between Notch and Hif- α in development and survival of *Drosophila* blood cells. *Science*. 2011;332(6034):1210-3.

108. Etet PFS, Vecchio L, Kamga PB, Nukenine EN, Krampera M, Kamdje AHN. Normal hematopoiesis and hematologic malignancies: role of canonical Wnt signaling pathway and stromal microenvironment. *Biochimica et Biophysica Acta (BBA)-Reviews on Cancer*. 2013;1835(1):1-10.
109. Owusu-Ansah E, Banerjee U. Reactive oxygen species prime *Drosophila* haematopoietic progenitors for differentiation. *Nature*. 2009;461(7263):537.
110. Tothova Z, Kollipara R, Huntly BJ, Lee BH, Castrillon DH, Cullen DE, et al. FoxOs are critical mediators of hematopoietic stem cell resistance to physiologic oxidative stress. *Cell*. 2007;128(2):325-39.
111. Hatlen MA, Wang L, Nimer SD. AML1-ETO driven acute leukemia: insights into pathogenesis and potential therapeutic approaches. *Frontiers of medicine*. 2012;6(3):248-62.
112. BRIDGES C, BREHME K. The mutants of *Drosophila melanogaster*. With foreword by TH Morgan. *The mutants of Drosophila melanogaster With foreword by TH Morgan*. 1944(552).
113. Humbert P, Grzeschik N, Brumby A, Galea R, Elsum I, Richardson H. Control of tumorigenesis by the Scribble/Dlg/Lgl polarity module. *Oncogene*. 2008;27(55):6888.
114. Enomoto M, Igaki T. Deciphering tumor-suppressor signaling in flies: genetic link between Scribble/Dlg/Lgl and the Hippo pathways. *Journal of Genetics and Genomics*. 2011;38(10):461-70.
115. Pagliarini RA, Xu T. A genetic screen in *Drosophila* for metastatic behavior. *Science*. 2003;302(5648):1227-31.
116. Gateff E. Malignant neoplasms of genetic origin in *Drosophila melanogaster*. *Science*. 1978;200(4349):1448-59.
117. Beaucher M, Goodliffe J, Hersperger E, Trunova S, Frydman H, Shearn A. *Drosophila* brain tumor metastases express both neuronal and glial cell type markers. *Developmental biology*. 2007;301(1):287-97.
118. Bangi E, Pitsouli C, Rahme LG, Cagan R, Apidianakis Y. Immune response to bacteria induces dissemination of Ras-activated *Drosophila* hindgut cells. *EMBO reports*. 2012;13(6):569-76.
119. Jiang H, Patel PH, Kohlmaier A, Grenley MO, McEwen DG, Edgar BA. Cytokine/Jak/Stat signaling mediates regeneration and homeostasis in the *Drosophila* midgut. *Cell*. 2009;137(7):1343-55.
120. Parisi F, Stefanatos RK, Strathdee K, Yu Y, Vidal M. Transformed epithelia trigger non-tissue-autonomous tumor suppressor response by adipocytes via activation of Toll and Eiger/TNF signaling. *Cell reports*. 2014;6(5):855-67.
121. Chiu H, Ring BC, Sorrentino RP, Kalamariz M, Garza D, Govind S. dUbc9 negatively regulates the Toll-NF- κ B pathways in larval hematopoiesis and drosomycin activation in *Drosophila*. *Developmental biology*. 2005;288(1):60-72.
122. Arefin B, Kunc M, Krautz R, Theopold U. The Immune phenotype of three *Drosophila* leukemia models. *G3: Genes, Genomes, Genetics*. 2017;7(7):2139-49.
123. Araki M, Kurihara M, Kinoshita S, Awane R, Sato T, Ohkawa Y, et al. Anti-tumour effects of antimicrobial peptides, components of the innate immune system, against

haematopoietic tumours in *Drosophila* mxc mutants. *Disease models & mechanisms*. 2019;12(6):dmm037721.

124. Evans CJ, Liu T, Banerjee U. *Drosophila* hematopoiesis: Markers and methods for molecular genetic analysis. *Methods (San Diego, Calif)*. 2014;68(1):242-51.

125. Al Outa A, Abubaker D, Bazarbachi A, El Sabban M, Shirinian M, Nasr R. Validation of a *Drosophila* model of wild type and T315I mutated BCR-ABL1 in chronic myeloid leukemia: An effective platform for treatment screening. *Haematologica*. 2019:haematol.2019.219394.

126. Ghigliione C, Devergne O, Georgenthum E, Carballès F, Médioni C, Cerezo D, et al. The *Drosophila* cytokine receptor Domeless controls border cell migration and epithelial polarization during oogenesis. *Development*. 2002;129(23):5437-47.

127. Ayyar S, Pistillo D, Calleja M, Brookfield A, Gittins K, Goldstone C, et al. NF-kappaB/Rel-mediated regulation of the neural fate in *Drosophila*. *PloS one* U6 - ctx_ver=Z3988-2004&ctx_enc=info%3Aofi%2Fenc%3AUTF-8&rft_id=info%3Aid%2Fsummonserialsolutionscom&rft_val_fmt=info%3Aofi%2Ffmt%3Akev%3Amtx%3Ajournal&rftgenre=article&rftatitle=NF-kappaB%2FRel-mediated+regulation+of+the+neural+fate+in+Drosophila&rftjtitle=PloS+one&rftdate=2007-11-14&rftissn=1932-6203&rftvolume=2&rftissue=11&rftspage=e1178&rftepage=e1178¶mdict=en-US U7 - Journal Article. 2007;2(11):e1178-e.

128. Maxton KuchenmeisterMaxton K, Handel K, Schmidt-Ott U, Roth S, JackleJäckle H. Toll homologue expression in the beetle *tribolium* suggests a different mode of dorsoventral patterning than in *drosophila* embryos. *Mechanisms of development*. 1999;83(1-2):107.

129. Duffy JB. GAL4 system in *Drosophila*: A fly geneticist's Swiss army knife. *GENESIS*. 2002;34(1-2):1-15.

130. Shehab M, Sherri N, Hussein H, Salloum N, Rahal EA. Endosomal Toll-Like Receptors (TLRs) mediate enhancement of IL-17A production triggered by Epstein-Barr virus (EBV) DNA in mice. *Journal of Virology*. 2019:JVI. 00987-19.

131. Sherri N, Salloum N, Mouawad C, Haidar-Ahmad N, Shirinian M, Rahal EA. Epstein-Barr virus DNA enhances dipterin expression and increases hemocyte numbers in *Drosophila melanogaster* via the immune deficiency pathway. *Frontiers in microbiology*. 2018;9:1268.

132. Livak KJ, Schmittgen TD. Analysis of relative gene expression data using real-time quantitative PCR and the 2⁻ ΔΔCT method. *methods*. 2001;25(4):402-8.

133. Foley SB, Hildenbrand ZL, Soyombo AA, Magee JA, Wu Y, Oravec-Wilson KI, et al. Expression of BCR/ABL p210 from a knockin allele enhances bone marrow engraftment without inducing neoplasia. *Cell reports*. 2013;5(1):51-60.

134. Skaggs BJ, Gorre ME, Ryvkin A, Burgess MR, Xie Y, Han Y, et al. Phosphorylation of the ATP-binding loop directs oncogenicity of drug-resistant BCR-ABL mutants. *Proceedings of the National Academy of Sciences*. 2006;103(51):19466-71.

135. Chen M, Turhan AG, Ding H, Lin Q, Meng K, Jiang X. Targeting BCR-ABL+ stem/progenitor cells and BCR-ABL-T315I mutant cells by effective inhibition of the BCR-ABL-Tyr177-GRB2 complex. *Oncotarget*. 2017;8(27):43662.

136. Nicolini FE, Grockowiak E, Maguer-Satta V. T315I+ tyrosine-kinase independent CML cells resistance. *Oncotarget*. 2017;8(27):43600-1.
137. Ragab A, Buechling T, Gesellchen V, Spirohn K, Boettcher A-L, Boutros M. Drosophila Ras/MAPK signalling regulates innate immune responses in immune and intestinal stem cells. *The EMBO journal*. 2011;30(6):1123-36.
138. Turco M, Romano M, Petrella A, Bisogni R, Tassone P, Venuta S. NF- κ B/Rel-mediated regulation of apoptosis in hematologic malignancies and normal hematopoietic progenitors. *Leukemia*. 2004;18(1):11.
139. Chen R, Alvero AB, Silasi DA, Mor G. Inflammation, Cancer and Chemoresistance: Taking Advantage of the Toll-Like Receptor Signaling Pathway. *American Journal of Reproductive Immunology*. 2007;57(2):93-107.
140. Warsch W, Walz C, Sexl V. JAK of all trades: JAK2-STAT5 as novel therapeutic targets in BCR-ABL1+ chronic myeloid leukemia. *Blood*. 2013;122(13):2167-2175. *Blood*. 2014;123(19):3056-.
141. Warmuth M, Simon N, Mitina O, Mathes R, Fabbro D, Manley PW, et al. Dual-specific Src and Abl kinase inhibitors, PP1 and CGP76030, inhibit growth and survival of cells expressing imatinib mesylate-resistant Bcr-Abl kinases. *Blood*. 2003;101(2):664-72.